2021

Final Report – Organics and Bacterial Reductions by Treatment BMPs

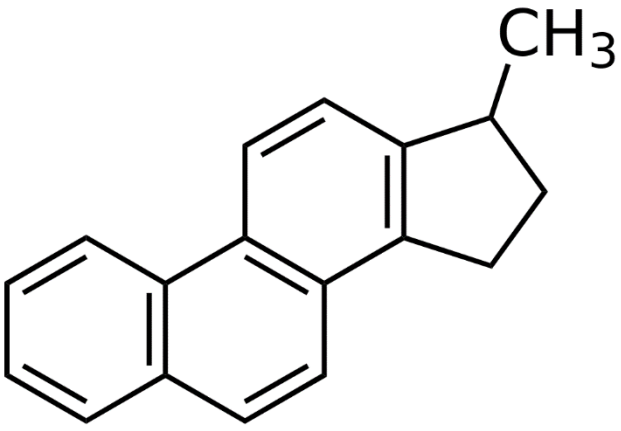

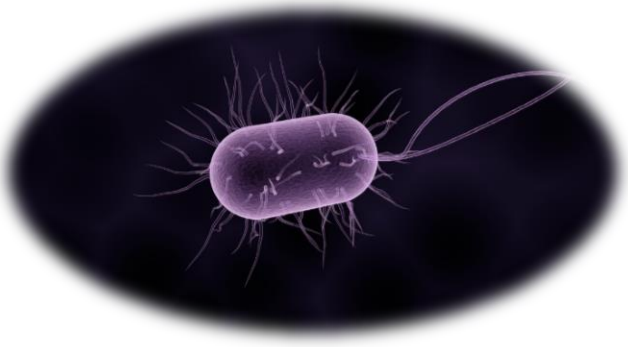

Anand Jayakaran, PhD PE

Chelsea Mitchell, MS

Washington State University

6/18/2021

Funding Acknowledgment

This project has been funded wholly or in part by the United States Environmental Protection Agency under assistance agreement 01J18101 to the Washington State Department of Ecology interagency agreement (IAA) IAA No. C1800116 between the State of Washington, Department of Ecology, and Washington State University.

CRediT[1] author statement

Anand Jayakaran, Principal investigator: Conceptualization, Methodology, Project supervision, Data analyses support, Writing- Reviewing and Editing.

Chelsea Mitchell, PhD Candidate: Conceptualization, Methodology, Sample collection, Data curation, Data analyses, Writing- Original & Final draft preparation, and all Visualization.

Other Acknowledgments

Brandon Boyd: developing sampling apparatus, assisting sample collection.

Carly Thompson, Andrew Flury: support with methodology, developing sampling apparatus, assisting sample collection.

We acknowledge the Washington State Department of Ecology personnel for managing and supporting this work and providing critical review and feedback.

[1] https://www.elsevier.com/authors/policies-and-guidelines/credit-author-statement

1 Executive Summary

Stormwater monitoring by Phase I municipal stormwater permittees in Western Washington from 2009-2013 confirmed a broad range of pollutants: solids, nutrients, metals, various organics including Polycyclic Aromatic Hydrocarbons (PAHs), pesticides, and fecal indicator bacteria (FIB) (Hobbs et al., 2015). Ecology's recommended treatment best management practices (BMPs) do not necessarily address the range of pollutants. Basic Treatment targets solids removal. Enhanced Treatment addresses solids and dissolved metals removal. Oil and phosphorus removal are also targeted.

The need for higher pollutant removals and BMPs addressing dissolved organics and bacteria is a priority for restoring Puget Sound. The Washington State Department of Ecology's 2019 Stormwater Management Manual for Western Washington does not have PAH and FIB standards that govern allowable limits in stormwater. Developing information useful towards developing such criteria is the overarching goal of this project. This work's primary objectives were to quantify PAH and FIB attenuation by specific bioretention soil media (BSM) through a bioretention column experiment.

Twelve large-scale columns were installed in a greenhouse at Washington State University's Puyallup Research and Extension Center. Four blends of bioretention mix comprising the standard bioretention mix of sand and compost (60:40 vol/vol), a blend comprising sand, compost, and biochar (60:20:20 vol/vol), and two blends of these two mixes inoculated with fungi. Stormwater was collected from a nearby highway bridge in Tacoma and used to dose the columns over EIGHT artificially dosed events. Influent and effluent concentrations of PAHs, FIBs, dissolved organic carbon (DOC), and total suspended solids (TSS) were measured in an analytical lab. PAHs and FIBs were also measured from the soil, sampled at two subsurface strata throughout the 18-month study. Samples were also collected from the surface once.

Results suggest higher concentrations of PAHs in compost alone, greater than the sum of what comes in via stormwater influent, and what leaves via effluent. Despite this result, total PAH concentrations in the soil reduced over time, a loss not explained by transport out of the system via effluent. We hypothesize that microbial activity reduced PAH concentration in the soils. DOC and TSS concentrations in the effluent also gradually diminished as the system aged.

The study showed that all four treatments comprising various blends of bioretention soil, biochar, and fungi effectively removed PAHs almost entirely from the influent stormwater. PAH removal was so successful that most effluent data comprised laboratory non-detects. A mixed-effects model was developed to explain how FIB, DOC, and TSS effluent concentrations varied jointly with influent contaminants. The statistical model suggested that columns amended with both biochar and fungi removed significantly more Fecal coliform than the BSM control columns. Bacteria concentrations in effluent samples were positively correlated with the concentrations of TSS in the effluent. Results also suggest that bacteria export from the columns were likely being transported via attachment to particles. DOC export was lower in biochar amended treatments than in treatments with the full 40% compost by volume. TSS removal was found to be significantly higher in the columns amended with both biochar and fungi.

2 Introduction

Organic and biological contaminants are widely detected in urban and peri-urban stormwater. Polycyclic Aromatic Hydrocarbons (PAHs) and Fecal Indicator Bacteria (FIB) are classes of organic and biological contaminants ubiquitous in stormwater that have known risks to human health and aquatic ecosystem integrity. Though these contaminants' sources and fate in stormwater differ, their removal mechanisms share similarities that may facilitate their simultaneous study. Studies have shown that PAHs and bacteria are removed from stormwater primarily by adsorption in the short term and are ultimately remediated by longer-term processes after adsorption to bioretention media or soils (DiBlasi et al., 2008, LeFevre et al., 2012a, 2012b, 2015). Bacteria are essential to the breakdown of PAHs, so the simultaneous attenuation of these contaminants likely requires a balance between fostering the growth of beneficial bacteria while promoting the inactivation of FIB.

The Washington State Department of Ecology's 2019 Stormwater Management Manual for Western Washington does not have PAHs and FIB standards that govern allowable limits in stormwater. Developing information that will be useful towards developing such criteria is the overarching goal of this project.

Though many studies nationwide have shown that PAH and FIB removal is possible using bioretention systems (Zhang et al., 2011; Chandrasena et al., 2014, Kim et al., 2012; Rusciano and Obropta 2007; Li et al., 2012), the published results show high variability, dependence on media used, influent flow and contaminant loading rates, and environmental conditions within the bioretention system. The variability in published results makes the extrapolation of results difficult, especially with the unique climate, soils, developmental pressures, and complex stormwater chemistry. It is important to note that while field evaluations of bioretention systems are important in furthering a broad understanding of factors that govern bioretention performance, developing a mechanistic understanding of PAH and FIB degradation factors can only be realized under controlled laboratory conditions. This study applied information derived from a year-long column study to real-world settings using a multivariable statistical framework to characterize how PAH and FIB degradation might occur in real-world bioretention systems.

2.1 PAHs

PAHs can be remediated in bioretention systems by adsorption to soil particles, microbial breakdown, and plant uptake (Haritash & Kaushik, 2009; LeFevre et al., 2011, 2012, 2015). Bioremediation of PAHs in soil is thought to be optimized in the presence of diverse soil microbial communities in which microbes work together to metabolize complex mixtures of PAHs and the intermediate metabolites which arise from their breakdown (El Amrani et al., 2015). This microbial co-metabolism is crucial for high molecular weight PAHs (>3 rings), which are rarely mineralized by a single microbial species (El Amrani et al., 2015). Chemical and physical interactions between plants, bacteria, and fungi can increase PAHs' bioavailability and bioremediation rates. This 'meta-remediation' by a consortium of biological kingdoms may be needed to optimize biodegradation (El Amrani et al., 2015).

Biodegradation of PAHs has been extensively studied in hydrocarbon contaminated soils. However, few studies have measured PAH biodegradation in stormwater bioretention systems

(LeFevre et al., 2011, 2012, 2015), which share many similarities with contaminated soils environments.

2.2 FIBs

Removal rates of pathogenic bacteria from stormwater are highly variable, and this variation has reportedly been explained by many factors, including loading rates, bioretention media, temperature, pH, pathogen species, and bioretention design. Once bacteria are retained in bioretention media, they can ultimately be remediated by die-off caused by the ecological conditions of the system such as pH (Benham et al., 2006), temperature (Howell et al., 1996; Selvakumar et al., 2007; Vidovic et al., 2007), wet-dry cycles (Li et al., 2016), and predation by other microorganisms (Zhang et al., 2010). If the adsorption of bacterial pathogens within bioretention systems is too weak, pathogens may desorb and be released in the effluent (Mohanty et al., 2014). Studies have suggested that sorptive geomedia, such as biochar and activated charcoal, can improve bacteria's removal and adsorption strength in bioretention systems (Mohanty & Boehm, 2014). Other media amendments can harness FIB inactivation using positively charged surfaces such as iron-oxide coated sands (Ryan et al., 2002; Zhang et al., 2010).

Optimizing PAHs and FIB removal from stormwater requires evaluating bioretention system design components that improve short-term removal and long-term remediation. Short-term removal for PAHs and FIB depends on the adsorptive capacity of the bioretention system. Long-term removal of PAHs is primarily driven by bioremediation performed by the system's resident microbial community. Long-term removal of harmful bacteria depends on the system's ability to retain and inactivate bacteria, which can be accomplished through predation, inactivation by charged media, or manipulation of environmental conditions.

A bioretention column study was developed to identify design modifications that optimize PAH and FIB removal from stormwater runoff. The data obtained from this study was used to build a multivariable statistical model that predicts target contaminant concentrations in BMP effluent from bioretention design metrics, system conditions (soil moisture and temperature), and contaminant loading rates. The multivariable model was then updated using influent contaminant concentration data from existing LID field sites and Western Washington stormwater contaminant concentrations reported in Western Washington NPDES Phase 1 Stormwater Permit: Final Data Characterization 2009-2013 (Hobbs et al., 2015).

This hybrid approach column-scale experiments and statistical modeling will inform BMP recommendation for PAHs and FIBs by: 1) generating data on removal efficiencies of planted bioretention systems amended with fungi and/or biochar, and 2) establish quantitative links between these bioretention design components and PAH and FIB removal efficiencies.

2.3 Study area and surroundings

The work will be carried out at the Washington State University Puyallup Research and Extension Center (WSU-P) located in the South Puget Sound. Stormwater for the studies at WSU-P will be collected from one of two potential sites in the South Puget Sound region.

2.3.1 History of the study area

The South Puget Sound region has undergone urbanization with considerable increases in impervious surface area and traffic volume. Stormwater runoff from these impervious surfaces transports metals, nutrients, PAHs, FIBs, and numerous emerging contaminants into streams draining to the Puget Sound estuary. Contaminant loading from stormwater is responsible for adverse ecological impacts on local aquatic habitats, such as decreased Index of Biological Integrity (IBI) scores and coho salmon pre-spawn mortality syndrome (Feist et al., 2017; Spromberg et al., 2015). Of these contaminants, PAH and FIBs are known pollutants of concern.

The primary mechanisms by which PAHs are removed from stormwater are sorption and biodegradation. The relative effectiveness of these mechanisms at attenuating PAHs depends on the molecular weight of the PAHs present. The bioavailability and solubility of PAHs decrease with increasing molecular weight (Johnsen et al., 2005). High molecular weight (HMW) PAHs with 4 or more rings (e.g., benzo[a]pyrene) sorb readily to hydrophobic materials, and therefore are easily removed from stormwater through sorption processes (Boving & Neary, 2007). Conversely, low molecular weight (LMW) PAHs with 3 or fewer rings (e.g., naphthalene) have higher bioavailability and thus are more readily degraded or biotransformed by microorganisms (Johnsen et al., 2005). LMW PAHs may still sorb to particles, but they have a lower affinity for the particle-associated state than HMW PAHs.

Several studies have documented the effectiveness of bioretention for removing PAHs from stormwater. McIntyre et al. (2015) observed a >92% reduction in total PAHs from stormwater treated by mesocosm scale bioretention columns. Similarly, DiBlasi et al. (2008) found that a field bioretention cell reduced the mass PAH load from stormwater by 87% on average. Lefevre et al. (2012a) found that lab-scale planted bioretention columns could remove up to 93% of naphthalene from synthetic stormwater, and unplanted columns could remove up to 73%. Previous studies have reported variable rates of FIB removal from stormwater using bioretention and various filtration media. Removal of FIB from stormwater is driven by several interacting processes, including environmental conditions, filtration, adsorption, and predation. Die-off rates of FIB in stormwater can be increased by 12-53% in the presence of light (Selvakumar et al., 2007), though complete die-off is expected to require several days of light exposure (Kinnaman et al., 2012), which is unrealistic for most stormwater BMPs. Other environmental conditions such as lack of nutrients (Vidovic et al., 2007) and low moisture (Ceustermans et al., 2007) can increase FIB die-off rates.

Bioretention has demonstrated an ability to reduce stormwater FIB loads with variable effectiveness. Some studies have reported improvements in FIB removal with the addition of plants to bioretention (Chandrasena et al., 2014), while others have reported lower removal rates in planted bioretention systems compared with unplanted systems (Kim et al., 2012). The addition of high surface area or charged media to stormwater filtration systems has improved FIB removal. For example, the addition of a positively charged media to sand, silt, and clay filter increased E. coli removal from 82% to 99% (Zhang et al., 2010). The addition of biochar (a high surface area geomedia) to a sand filter increased average E. coli removal from 35% (± 6 %) to 95% (± 1 %) and maintained high removal rates at a range of E. coli influent concentrations.

2.4 Project objectives

1. Carry out a bioretention column experiment using media, plants, and fungi in a factorial design, and test PAH and FIB removal at a mesocosm scale.
2. Use PAH and FIB removal by specific media, plant, and fungi combinations to ascertain their contributions to PAH and FIB removal under controlled conditions.
3. Extrapolate laboratory biogeochemical performance to real-world conditions using a multivariable statistical framework with existing field-derived influent data.

3 Methods

3.1 Parameters of interest

The contaminants of interest for this project are Polycyclic Aromatic Hydrocarbons (PAHs, Table 1), Fecal Coliform, and *Escherichia coli* (*E. coli*).

Table 1. PAH analytes that were analyzed in water and soil for this study.

PAH analytes*	**Abbrev.**	**CAS**	**Sample type**	
			water	**soil**
Naphthalene	NPTH	91-20-3	x	x
2-Methylnaphthalene	2MNPT	91-57-6	x	x
1-Methylnaphthalene	1MNPT	90-12-0	x	x
Acenaphthylene	ACY	208-96-8	x	x
Acenaphthene	ACE	83-32-9	x	x
Dibenzofuran	DF	132-64-9	x	x
Fluorene	FLU	86-73-7	x	x
Phenanthrene	PHN	85-01-8	x	x
Anthracene	ANT	120-12-7	x	x
Carbazole	CA	86-74-8	x	
Fluoranthene	FLA	206-44-0	x	x
Pyrene	PYR	129-00-0	x	x
Benzo[a]anthracene	BAA	56-55-3	x	x
Chrysene	CHR	218-01-9	x	x
Benzo(b)fluoranthene	BBF	205-99-2	x	x
Benzo(k)fluoranthene	BKF	207-08-9	x	x
Benzo(j)fluoranthene	BJF	205-82-3	x	x
Benzofluoranthenes,Total (b+k+j)ǂ	BFT		x	x
Benzo(a)pyrene	BAP	50-32-8	x	x
Indeno(1,2,3-cd) pyrene	IDP	193-39-5	x	x
Dibenzo(a,h) anthracene	DBA	53-70-3	x	x
Benzo(g,h,i) perylene	BZP	191-24-2	x	x

* The 21PAH analytes listed above are the suite of PAHs analyzed and reported by Analytical Resources, Inc using GC/MS (8270D). X's indicate PAH compounds which ARI is accredited to analyze in water and soil samples using this method.

ǂTotal Benzofluoranthenes is calculated as the sum of the individual benzofluoranthene (b+j+k) peaks.

3.2 Project overview

Given the reasonably small body of work and dearth of BMPs that are specifically designed to treat PAHs and FIBs in stormwater, this project first aims to evaluate emerging bioretention design components that may affect PAH and FIB removal. A controlled bioretention column study with a factorial design was used to accomplish this goal. The emerging design components evaluated in this study included ligninolytic fungi and biochar to planted bioretention soil. Bioretention columns located inside a greenhouse were dosed with field-collected highway runoff. PAH and FIB removal efficiencies were determined through chemical and microbial analysis of the influent and effluent. In addition, PAHs within the bioretention columns throughout the study were tracked via PAH analysis of bioretention soils. The timeline of tasks completed for this study is shown below (Figure 1).

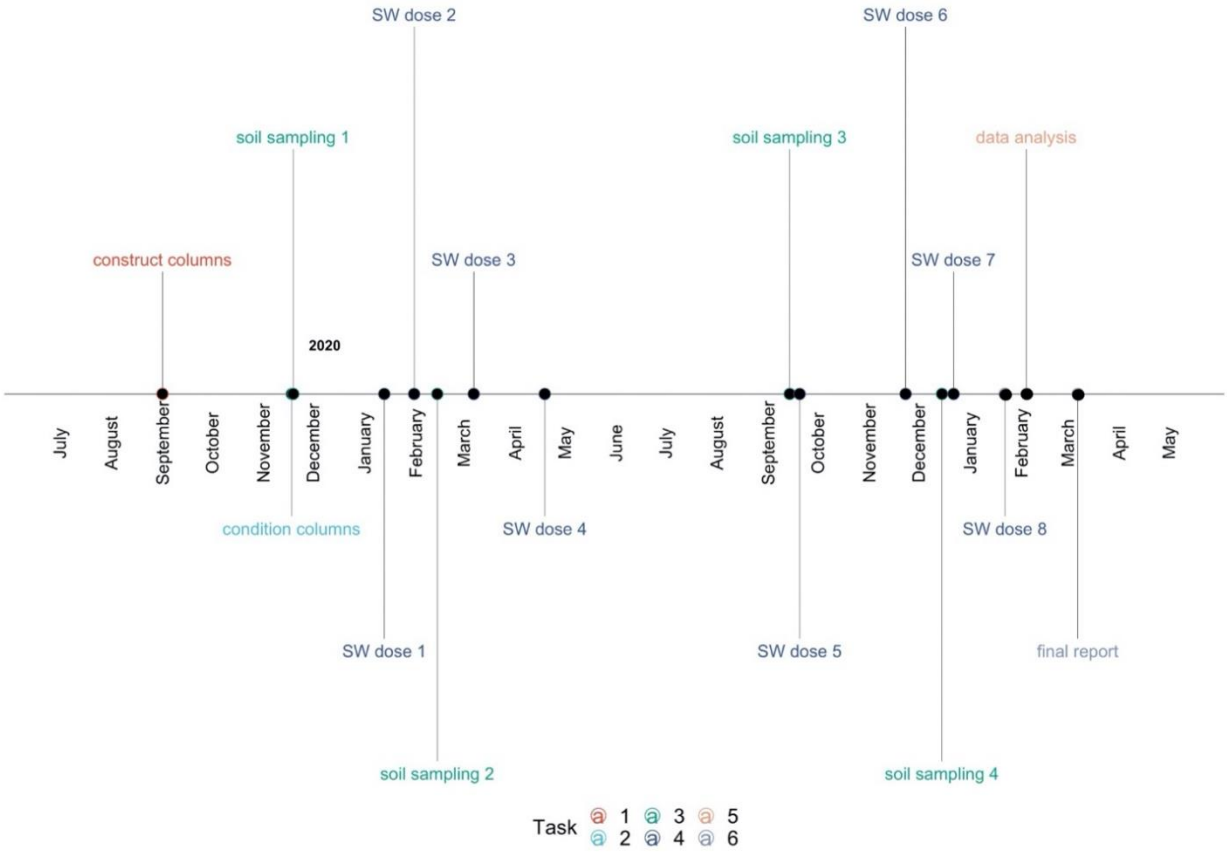

Figure 1. Timeline of project tasks.

3.3 Experimental design

3.3.1 Stormwater collection

Stormwater for the dosing was collected from a downspout at the junction of I-5 with SR-16 in Tacoma (Figure 2). Runoff from the downspout was collected in a 500 gal HPDE tank and transferred into a 250 gal stainless steel tote for transport back to WSU-P. The stormwater collected in the HPDE tank was recirculated for 10 minutes to resuspend sediments and then

Figure 2. A) Stormwater runoff sampling site location in Tacoma, WA off the junction of I-5 and SR-16. B) Pumping stormwater from the HPDE collection tank into a stainless-steel transfer tank. C) The collection tank collecting water from the highway runoff downspout.

pumped via an outlet drain at the bottom of the tank into a stainless-steel tote. This collection

process appeared to retain a majority of the sediments in the highway runoff, however the proportion of sediments retained was not measured. To prevent stormwater and sediments from accumulating between events, the tank was moved away from the downsout and the underdrain valve on the collection tank was left open. Sediment that was not transferred during pumping, remained in the HPDE tote. The collection tank was cleaned every 2-3 months as needed to prevent the accumulation of sediments and debris. Stormwater was used to dose bioretention columns within 48 hours after the stormwater collection began.

During stormwater collection, a grab sample of the highway runoff was taken from the collection tanks and stored on ice to be analyzed for PAHs, E. coli, F.C., TSS, and DOC. The temperature was taken from the filled stormwater tote after collecting the field grab samples and at the end of column dosing. Temperatures varied by about 5C between collection and dosing. A recirculating flow system was built to maintain a homogeneous mixture in the stormwater tote during column dosing.

3.3.2 Column design

A factorial bioretention column experimental design was chosen to test the effects of adding biochar and/or fungi to a typical bioretention cell (Table 2). Biochar and fungi were chosen as factor levels for this experiment based on a literature review conducted for this project. Published studies showed evidence that both biochar and fungi may effectively remove PAHs and FIBs from stormwater and stimulate PAH bioremediation within bioretention columns. In addition, the experimental design included plants in all columns because plants are typically found in bioretention cells, and because plants have been shown to improve the removal of PAHs (LeFevre et al., 2018) and bacteria (Chandrasena et al., 2014) in bioretention systems.

A PVC column design was selected because it was cost and space-efficient and comparable with many published methods for evaluating bioretention performance (Zhang et al.,2010, Kim et al.,2012, Chandrasena et al.,2014, McIntyre et al.,2015, Spromberg et al.,2015). Large (36" height, 15" diameter) PVC columns planted with *Carex oshimensis* were filled with a 60:40 (by volume) Sand:Compost mixture (Figure 3).

Table 2. Descriptions of bioretention treatments in the experiment.

Treatment label	N	Description*
BSM control	3	Bioretention soil (60% sand, 40% compost)
BSM + BC	3	Bioretention soil with biochar (60% sand, 20% compost, 20% biochar)
BSM + FUNGI	3	Bioretention soil, inoculated with *Stropharia rugosoannulata*
BSM + BC + FUNGI	3	Bioretention soil with biochar (60% sand, 20% compost, 20% biochar), inoculated with *Stropharia rugosoannulata*

*all columns were planted with *Carex oshimensis* (common name: Evergold).

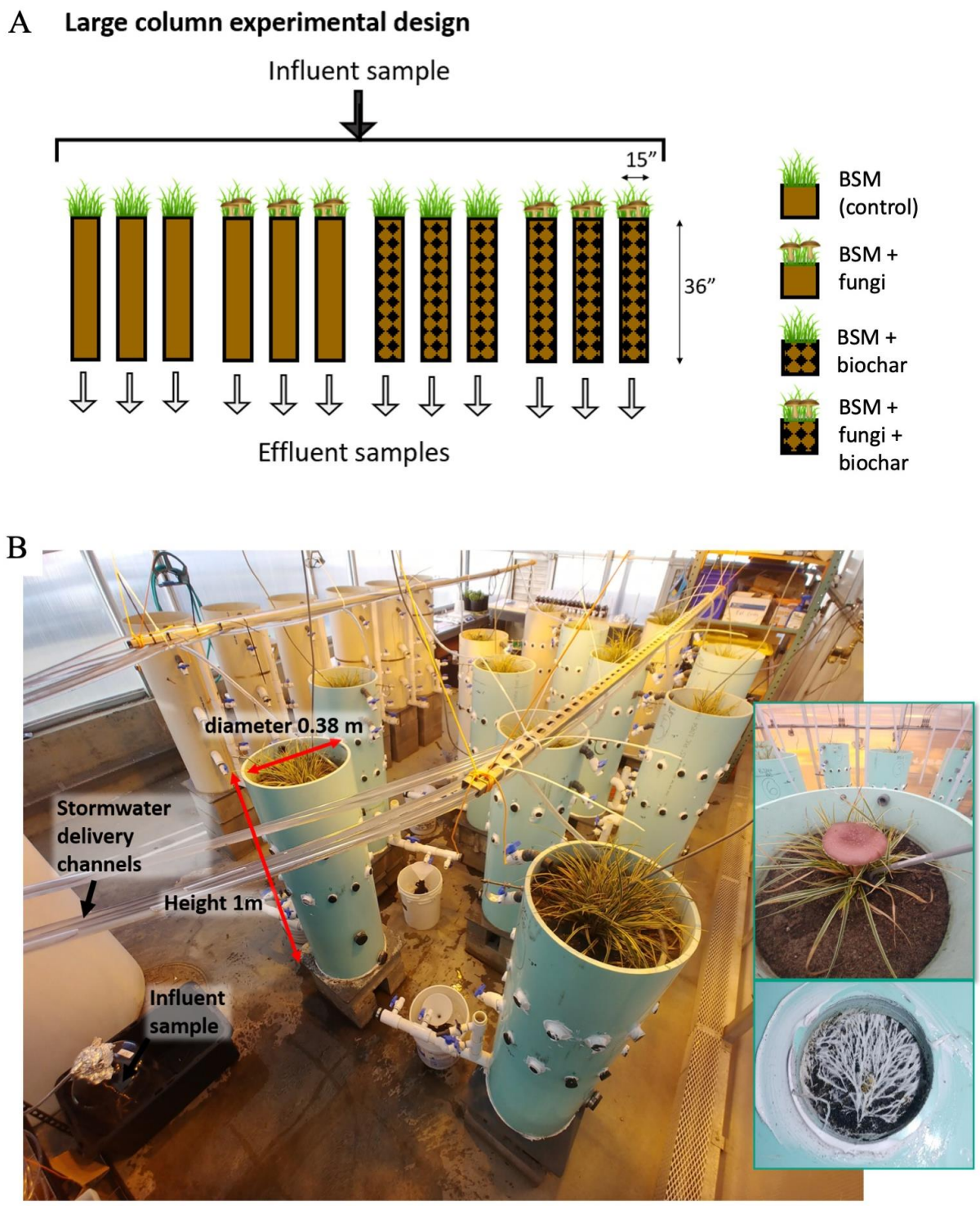

Figure 3. A) Bioretention column experimental design, and B) picture of experimental setup in greenhouse at WSU-Puyallup.

3.4 Water sampling

Eight storm events were sampled over the course of one year (Figure 1). Bioretention columns were dosed with highway stormwater runoff at 18L/hour for 3 hours during each event. This resulted in each column being dosed with 54 L of influent water during each event.

Stormwater was collected from a downspout off SR-16 in Tacoma, WA (Figure 2) and transported in a stainless-steel tote to WSU-P. Water samples from each column's effluent and a composite of the influent were collected for laboratory analysis. Samples of untreated (influent) and treated (effluent) stormwater were sent to two Ecology accredited laboratories for analytical analyses: Spectra laboratories (*E. coli* and Fecal coliform) in Tacoma, WA and Analytical Resources, Inc. (PAHs, TSS, and DOC) in Tukwila, WA.

3.5 Bioretention media sampling

Between stormwater dosing events, the bioretention soils in each column were non-destructively sampled for soil PAHs. Soil samples were taken at two depths in each column – A) 6" deep at the middle of the rhizosphere (i.e., the zone of soil influenced by plant roots), and B) 11" deep at the bottom depth of the BSM control (Figure 4). PAH degradation activity was expected to be elevated in the rhizosphere because of the complex interactions between plant root exudates, bacteria, and fungal hyphae. Therefore, analysis of PAH concentrations in the bottom depth of the BSM control was expected to inform the extent to which PAH degradation occurs at depth in bioretention systems.

Soil samples were taken after two stormwater dosing events. Therefore, the total % volume of each column extracted for soil samples throughout the experiment was < 4 %.

Soil samples were extracted horizontally from each column from pre-drilled holes at each depth using a 3/4" soil core sampler extending no more than 7" towards the center of the column (Figure 4). Holes were plugged with rubber stoppers when not being sampled.

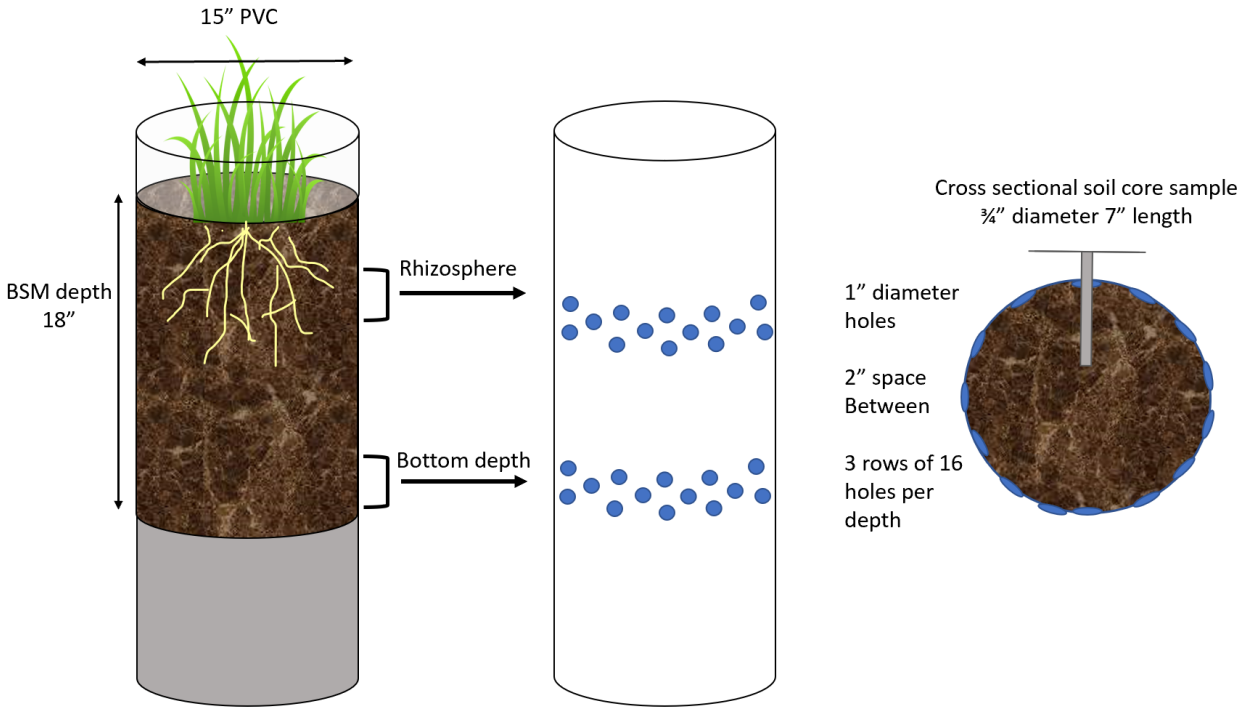

Figure 4. Design for sampling soil non-destructively from bioretention columns at 2 depths.

3.6 Media temperature and moisture content sensing

Media moisture and temperature were measured using 12 multi-segment soil moisture and temperature profile probes, inserted down every column's center (GroPoint™ Profiling 8 Segment Probe, GroPoint, Vancouver BC). Probes were calibrated by the manufacturer in precisely set dielectric solutions. The dielectric solutions emulated a moderate loamy soil at volumetric moisture contents of 7.9% and 41.0% volumetric moisture content (VMC). Dielectric and volumetric moisture values were determined with a reference Stevens Hydraprobe instrument. Probes were calibrated to ensure that each measurement segment provides readings that match to within ±0.5% of the "dry" and "wet" solutions equivalent volumetric moisture content levels. Inter-sensor variability was expected to be less than 1% variance, typically +-0.5%. The sensor was designed to measure soil moisture and temperature at discrete depths, incrementing at 15 cm intervals. This allowed for measuring conditions within the column from the rhizosphere to the bottom sampling zone shown in Figure 4.

Before installation, each probe was custom calibrated with the appropriate media following the manufacturer's recommended protocols. Briefly, this involved taking soil moisture readings at multiple moisture levels (dry to saturated) and comparing them with empirically determined volumetric moisture contents. Then, soil-specific calibration coefficients were determined by applying a polynomial fit to the results.

3.7 Statistical analysis:

To estimate the effect of bioretention treatment on contaminant removal rates, we fitted random intercept models to the data with dosing events considered a random effect. A random intercept model is a type of linear mixed-effects model which allows the intercept to vary based on a specified hierarchical data structure. The equation for a random intercept model is:

$$Y_{ij} = X\beta + Z_i b_i + \varepsilon$$

Y_{ij} *is* the effluent concentration for a given column j and event i; X is the categorical variable for treatment; and Z_i is the random effect of dosing event i on the intercept, b_i (Zuur et al., 2009). The intercept for the model is allowed to change for each dosing event, i. Treatment was coded so that the control bioretention media (BSM) was considered the reference level (level 0), while the other treatment levels (BSM+BC, BSM+FUNGI, and BSM+BC+FUNGI) were contrasted against the reference (level 1).

In this work, influent concentrations for any given dosing event were the same across all columns but varied widely amongst events. Since influent concentration is implicit in the calculation of removal efficiency, removal efficiencies for a given contaminant are likely to be more similar to each other within an event, than to removal rates amongst many events. This creates a hierarchical data structure that can be represented by Figure 5. In addition, by allowing the intercept in our models to vary by event, we can better distinguish variability in removal rates caused by treatment.

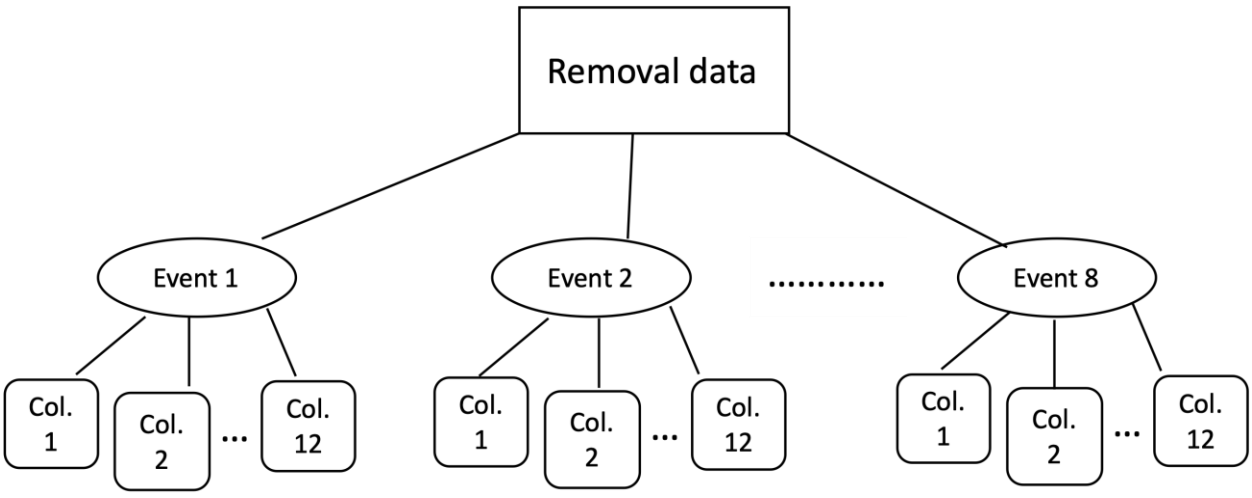

Figure 5. Diagram of the hierarchical data structure of contaminant removal rates for this study.

3.7.1 Censored data

3.7.1.1 Chemistry data

The majority of non-detect values in the chemistry dataset occurred in the PAH effluent data. PAH effluent data was non-detect ("U-qualified") in 98.3% of samples. Similarly, 47.9% of PAH influent data was censored. These high levels of non-detect data limit precluded use of imputation methods for handling censored data. PAHs were summed as Total PAHs (TPAHs) for calculating treatment performance. To facilitate calculating TPAHs for this purpose, we substituted 0 for non-detect values.

The DOC data contained only one U-qualified data point, and the TSS data contained only two U-qualified data points. Because non-detects were few in this dataset, the detection limits (TSS=1 mg/L, DOC=0.5 mg/L) were used for these observations.

3.7.1.2 Bacteria counts

Bacterial counts obtained through the membrane filtration (M.F.) method can be censored for several reasons (Table 3). When there is a growth of non-target organisms on the filter, this is known as confluent growth (C.G.). Confluent growth can prevent reliable counts of target organisms. Stormwater samples contain myriad species of bacteria, so C.G. is common for these samples. Second, if no growth occurs on a plate at any of the dilutions used, the sample value is flagged as "U-qualified." This is similar, but not equivalent, to a non-detect value in chemistry data. It does not mean that the sample contained no target microorganisms, but it does indicate that levels are low enough in the sample that no colony-forming units (CFU) grew on the filter. These U-qualified values were replaced with a numerical value of 1 (one) in our dataset to facilitate the log removal calculations used; we acknowledge that these values are not equivalent to non-detection (Table 3). Finally, in some cases, there can be too much growth on a filter to enable reliable bacteria counts. These values are marked as"> value" and are taken as the value estimate in our dataset.

Lab technicians who processed our samples noted that confluent growth was common in our samples. In addition, they noted that diluting samples any more than 1:2 produced blank plates (U-qualified) and using any more than 1 mL of sample produces too much confluent growth for enumeration. These constraints increased the likelihood of U-qualified results. Figures A1-A6 in the Appendix show pictures (provided by Spectra Laboratories) of Fecal coliform and *E. coli* plates from dosing event 4 samples from this study. The pictures show confluent growth and multiple dilutions.

Table 3. Types of censored values for microbiology data and the actions taken to manage these values.

Censor type	**Description**	**Action**
C.G.*	Confluent growth: Excessive growth of non-target organisms.	Omit from the analysis.
* value	Confluent growth on at least one dilution.	Retain result value as is.
** value	Results reported as an estimate due to confluent growth.	Retain result value as is.
< value, U-qualified	No growth	Substitute value with 1 (facilitates log removal calculations).
> value	Too many colonies for exact colony count.	Retain result value as is.

3.8 Mass balance

A mass balance of total PAHs was performed for each bioretention column to track PAH sources, fate, and transport. Total PAHs were measured in soil samples after initial column conditioning and then after stormwater dosing events 2, 4, and 6. Total PAHs were also measured in the influent (input) and effluent (export) for each stormwater dosing event. These total PAH concentrations were converted to mass values in soil or water by multiplying them by a given column's media mass or the volume of influent passing through columns during a given dosing event. Media weights for each column are provided in Table 4, and influent volume for each column during each event was assumed to be 54 L since columns were dosed at a rate of 18 L/hr for 3hrs.

For the mass balance analysis, we calculated initial total PAH mass (ug) in bioretention soils, the input of total PAHs via influent, export of total PAHs via effluent, net total PAHs added to bioretention soils via influent, end mass of total PAHs in bioretention soils, and the % mass lost in bioretention soils throughout the study. Each of these metrics was first calculated for each individual column and then summarized using a mean and standard deviation (n = 3) for each treatment.

Table 4. Bioretention column loading data includes total volume of media in the column, the total mass of media in the column, wet weight of *Carex* plants, and *Carex* plants' root length.

Column	**Media**	**Total volume (L)**	**Total mass of media (kg)**	**Plant wet wt. (kg)**	**Root length (cm)**
1	BSM+BC	58	61.57	0.15	31.8
2	BSM+BC	58	62.27	0.12	50.8
3	BSM	54	61.48	0.13	38.1
4	BSM	54	62.65	0.10	45.7
5	BSM	54	62.16	0.12	35.6
6	BSM+BC	58	64.30	0.10	40.6
7	BSM+BC	58	65.14	0.10	38.1
8	BSM+BC	58	64.13	0.07	31.8
9	BSM	54	62.45	0.08	53.3
10	BSM	54	65.64	0.12	30.5
11	BSM+BC	58	63.45	0.13	36.8
12	BSM	54	65.31	0.11	33.0
Mean			**63.38**	**0.11**	**38.8**
Std. dev			**1.49**	**0.02**	**7.5**

4 Results

Influent, stormwater grab samples, and column effluent samples were analyzed for 23 PAHs, Fecal coliform (M.F.), *E. coli*, Total Suspended Solids, and Dissolved Organic Carbon during each event. The BSM control fraction of PAHs was also analyzed in bioretention soils at shallow (6") and deep (11") soil strata, repeated four times throughout the study. Soil moisture and temperature data were logged continuously using segmented probes, though data loss was experienced during several periods. Results from these analyses are presented below. All PAH compounds, total suspended solids, and dissolved organic carbon were analyzed in water samples for 8 dosing events. Fecal coliform and *E. coli* were analyzed in only 7 dosing events because time constraints during dosing event 2 prevented microbiology samples from being transported to the lab within the proper holding time (6 hours).

4.1 Field stormwater contaminant profile

The target contaminants measured in the stormwater grab samples (Field S.W.) fall within the range of concentrations reported in the Western Washington NPDES Phase I Stormwater Permit (Hobbs et al., 2015). The most frequently detected PAHs in the present study were pyrene, fluoranthene, and phenanthrene, the same as the most commonly detected by Hobbs et al. (2015). Two-ring PAHs (e.g.,1-Methylnaphthalene, 2-Methylnaphthalene, and naphthalene) were detected much more frequently in our dataset than Hobbs et al. (2015) (Table 6). However, Hobbs et al. (2015) employed analytical testing with lower detection levels, increasing the likelihood of detection.

Table 5. Comparison of PAH analyte summary statistics between field stormwater grab samples and monitoring data from Hobbs et al. 2015.

Compound	Units	Concentration range	
		Hobbs 2015	Field SW
pyrene	µg/L	0.007-26	0.082-0.456
Fluoranthene	µg/L	0.007-33	0.052-0.324
Phenanthrene	µg/L	0.006-16	0.033-0.216
Chrysene	µg/L	0.003-16	0.026-0.173
Benzofluoranthene	µg/L	0.067-5.7	0.034-0.255
Benzo(g,h,i)perylene	µg/L	0.004-12	0.05-0.293
Benz(a)anthracene	µg/L	0.004-11	0.011-0.078
Naphthalene	µg/L	0.004-2.2	0.012-0.224
Benzo(b)fluoranthene	µg/L	0.02-13	0.021-0.143
Indeno(1,2,3-cd)Pyrene	µg/L	0.004-10	0.015-0.11
Benzo(a)pyrene	µg/L	0.004-15	0.011-0.112
Benzo(k)fluoranthene	µg/L	0.007-13	0.011-0.057
2-Methylnaphthalene	µg/L	0.003-2.5	0.011-0.074
Dibenzo(a,h)anthracene	µg/L	0.005-5.3	0.01-0.056
Fluorene	µg/L	0.003-1.6	0.01-0.056
Anthracene	µg/L	0.004-5.4	0.01-0.056
Acenaphthene	µg/L	0.003-1.5	0.01-0.056
Acenaphthylene	µg/L	0.003-1.5	0.01-0.056
1-Methylnaphthalene	µg/L	0.1-1.6	0.01-0.056
Carbazole	µg/L		0.011-0.056
Dibenzofuran	µg/L		0.01-0.056
Perylene	µg/L		0.011-0.056
Fecal coliform	CFU/100 mL	1-1,100,000	100-3000
E. coli	CFU/100 mL		200-1100
Total suspended solids	mg/L	1-4700	35-274

4.2 Analysis of treatment performance

4.2.1 Contaminant correlations

To examine the relationships between influent and effluent samples and to see how those relationships might change with bioretention treatment, correlations between influent and effluent samples were determined (Figure 6). P-values reported are corrected for multiple testing using Bonferroni's adjustment.

Influent samples with the highest positive correlations ($R = 0.97$, $p < 0.001$) were influent TSS ("inf_TSS") and TPAHs ("inf_PAH"), suggesting that the processes that deposit TSS and TPAHs on road decks and transports these to the influent collection point are similar. The correlative relationship between TPAH and TSS disappeared at the effluent stage, hinting at the idea that bioremediation disrupts the influent relationship, and that simple filtrative processes known to remove TSS possibly do not apply to TPAH removal.

Influent concentrations of Fecal coliform ("inf_FC") showed significant and inverse correlations with influent TPAHs ($R = -0.48$, $p < 0.01$) and influent TSS ($R = -0.42$, $p < 0.01$). Among influent samples, Fecal coliform and TSS concentrations were significantly and positively correlated ($R = 0.64$, $p < 0.01$). Influent DOC concentrations were inversely correlated to bioretention column age ("Age") ($R = -0.41$, $p < 0.01$).

Interestingly, influent Fecal coliform samples were positively correlated with influent ($R=0.30$, $p = 0.01$) AND effluent ($R = 0.57$, $p < 0.01$) *E. coli* concentrations.

Amongst effluent samples Fecal coliform concentrations were significantly correlated to TSS ($R = 0.64$, $p < 0.01$), DOC ($R = 0.36$, $p < 0.01$), and *E. coli* ($R = 0.34$, $p < 0.01$) concentrations in the effluent. Effluent DOC concentrations were also correlated with TSS in the effluent ($R = 0.42$, $p < 0.01$). Bioretention column age was negatively correlated with effluent TSS ($R = -0.73$, $p < 0.001$), effluent DOC ($R = 0.69$, $p < 0.001$), and effluent Fecal coliform ($R = -0.43$, $p < 0.001$) concentrations. Influent correlation between TSS and PAHs reflects PAH attachment to particles in stormwater.

Negative correlation between influent F.C. and TSS/PAHs may reflect Event 6 (12/17/20) where F.C. concentrations were very low while TSS and PAH concentrations were high. A high correlation between effluent TSS and F.C. suggests that particulate matter/TSS may transport F.C. Effluent TSS and DOC concentrations were both negatively correlated with age, suggesting these effluent concentrations diminish over time.

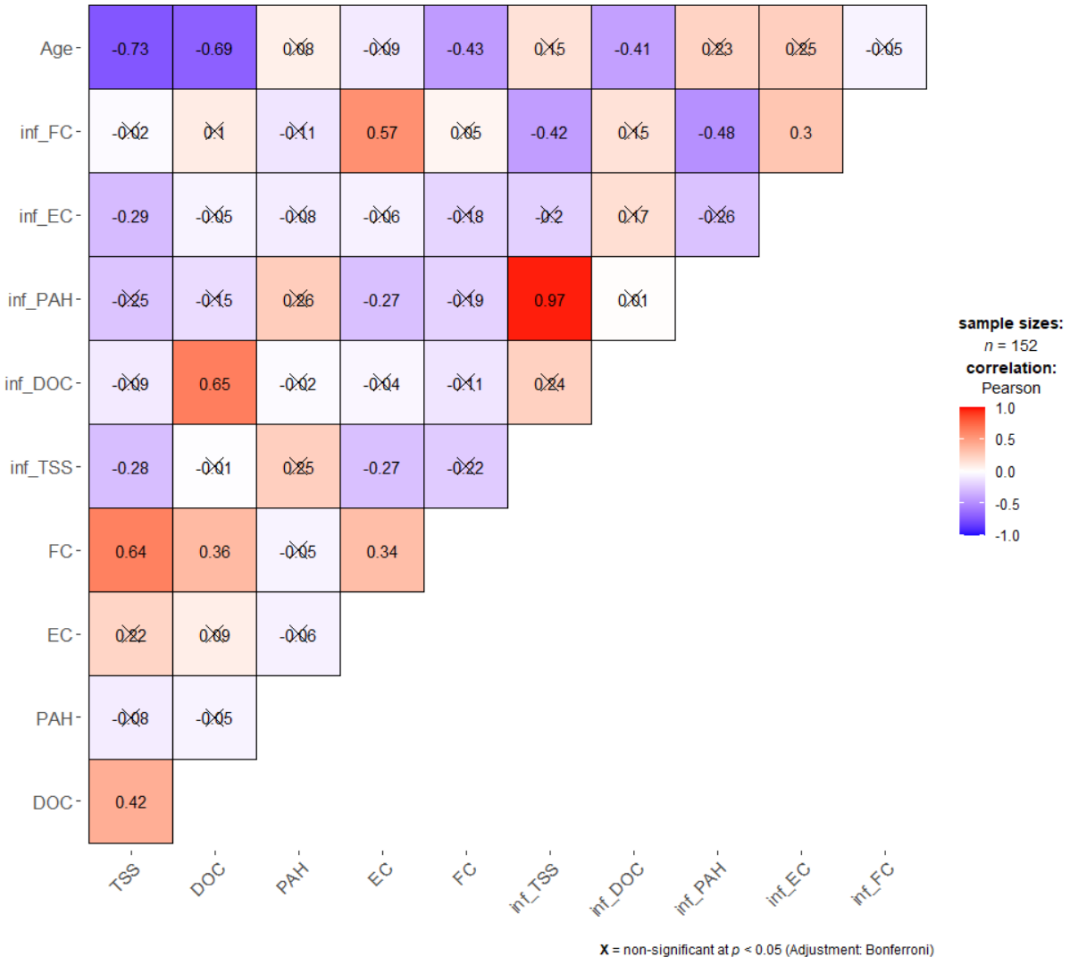

Figure 6. Correlation plots for influent and effluent samples. Positive correlations are shown in red while negative correlations are shown in blue. Darker shades represent stronger correlations. P-values were adjusted for multiple testing using Bonferroni corrections. Non-significant correlations are crossed out.

4.2.2 Treatment effects

Escherichia coli concentrations detected in the influent samples ranged from 22-1,300 CFU/100 mL with a median of 400 CFU/100 mL and a geomean of 348 CFU/100 mL (Figure 7). *E. coli* concentrations in the field stormwater grab samples ranged from 200-1,100 CFU/100 mL with a median of 600 CFU/100 mL and a geomean of 558 CFU/100 mL. For effluent samples, *E. coli* concentration geomeans were 323 CFU/ 100 mL (BSM control), 132 CFU/100 mL (BSM + BC), 159 CFU/100 mL (BSM + BC + FUNGI), and 203 CFU/100 mL (BSM + FUNGI).

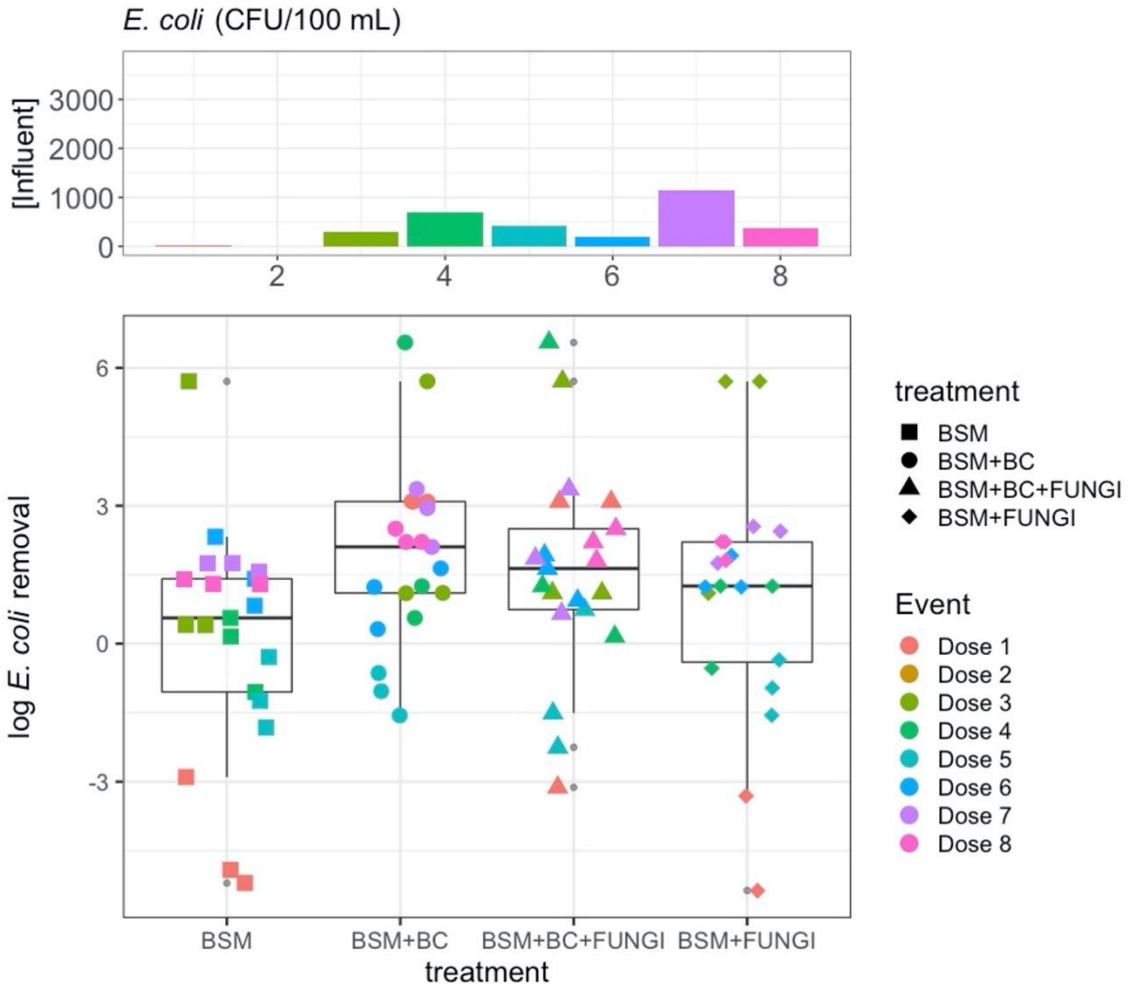

Figure 7. (Top) Influent concentrations for each dosing event, and (bottom) corresponding natural log removal rates for each treatment pooled across all dosing events. Data were not available for event 2.

Fecal coliform concentrations detected in the influent samples ranged from 150-4,200 CFU/ 100 mL with a median of 900 CFU/ 100 mL and a geomean of 896 CFU/ 100 mL. Fecal coliform concentrations in the field stormwater grab samples ranged from 400-3,000 CFU/ 100 mL with a median of 800 CFU/ 100 mL and a geomean of 863 CFU/ 100 mL. In general, effluent Fecal coliform concentrations were lower than influent and field stormwater concentrations after dosing event 3 (Figure 8). For effluent samples, Fecal coliform concentration geomeans were

535 CFU/ 100 mL (BSM control), 346 CFU/ 100 mL (BSM + BC), 275 CFU/ 100 mL (BSM + BC + FUNGI), and 270 CFU/ 100 mL (BSM + FUNGI).

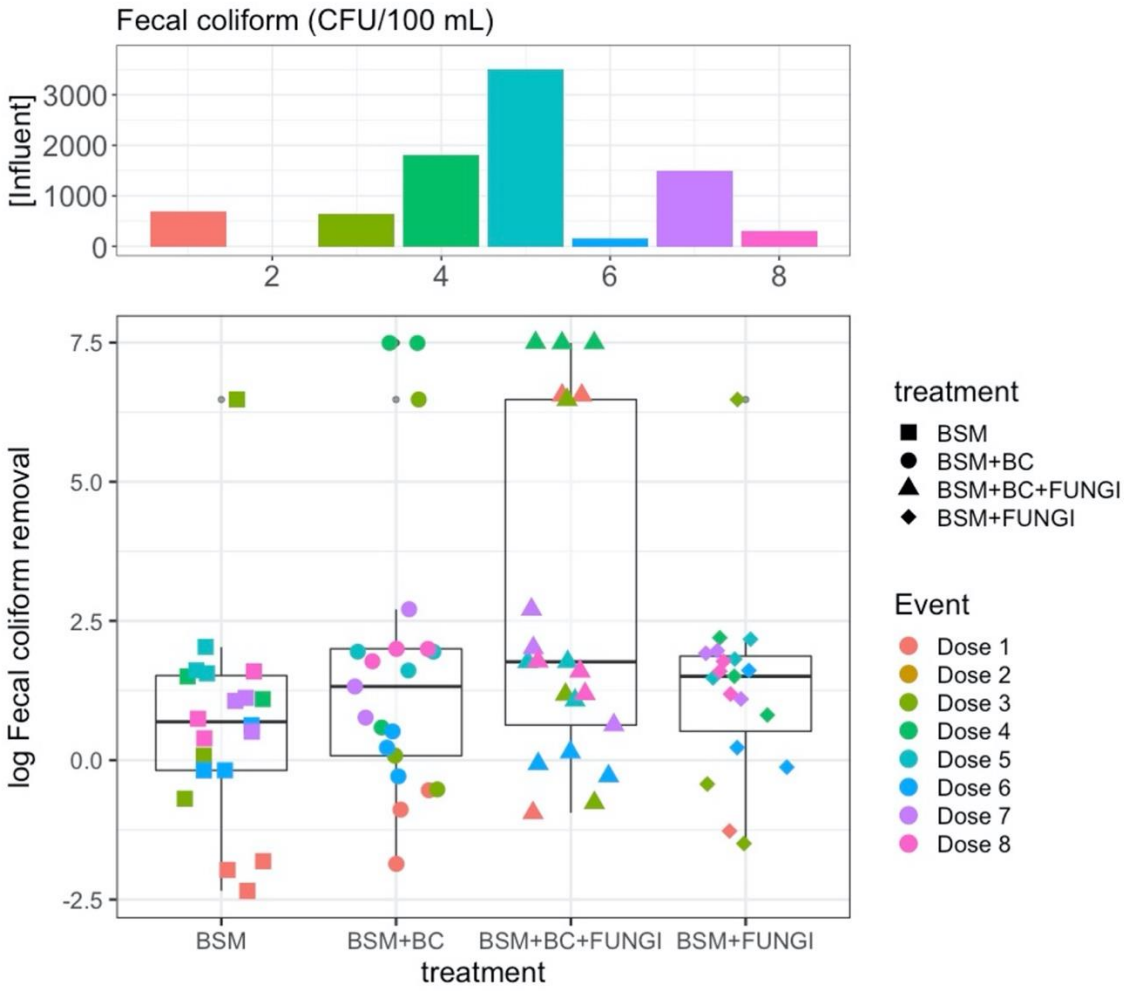

Figure 8. (Top) Influent concentrations for each dosing event, and (bottom) corresponding natural log removal rates for each treatment pooled across all dosing events. Data were not available for event 2.

Total PAHs were removed efficiently from stormwater with percent removal rates >97% in 94 of 96 samples (Figure 9). During dosing event 6, column 10 (BSM control) removed only 61.8% of Total PAHs, but this appears to be an outlier. Similarly, during event 8, column 2 removed only 82% of Total PAHs. Influent total PAH concentrations ranged from 0.089-4.62 ug/L with a median of 0.64 µg/L and a geomean of 0.66. The most abundant PAHs in influent samples were pyrene (15.2%), fluoranthene (13.1%), phenanthrene (9.1%), and Total benzofluoranthenes (8.7%). Most effluent PAHs were non-detect, regardless of treatment. No one bioretention amendment outperformed another.

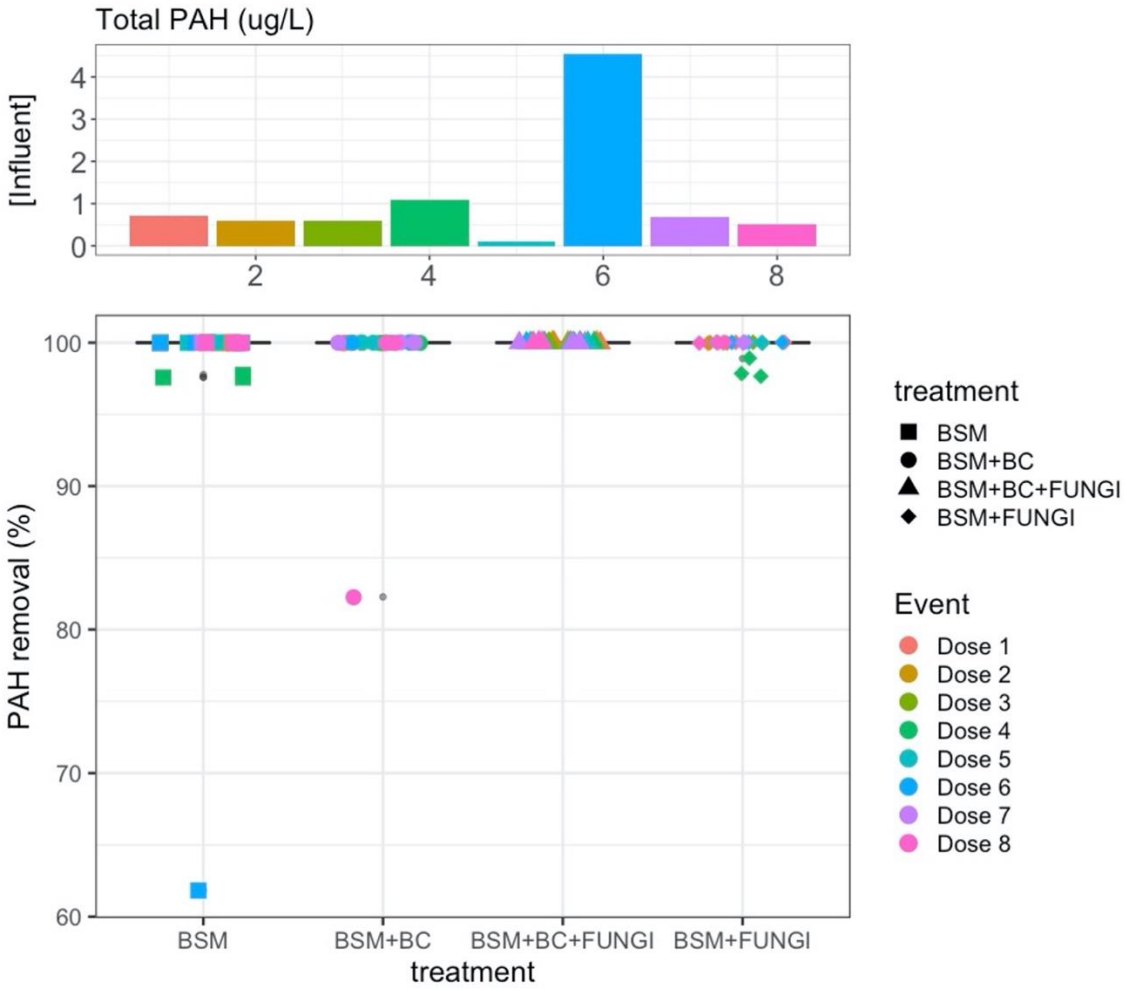

Figure 9. (Top) Influent concentrations for each dosing event, and (bottom) corresponding percent removal rates for each treatment pooled across all dosing events.

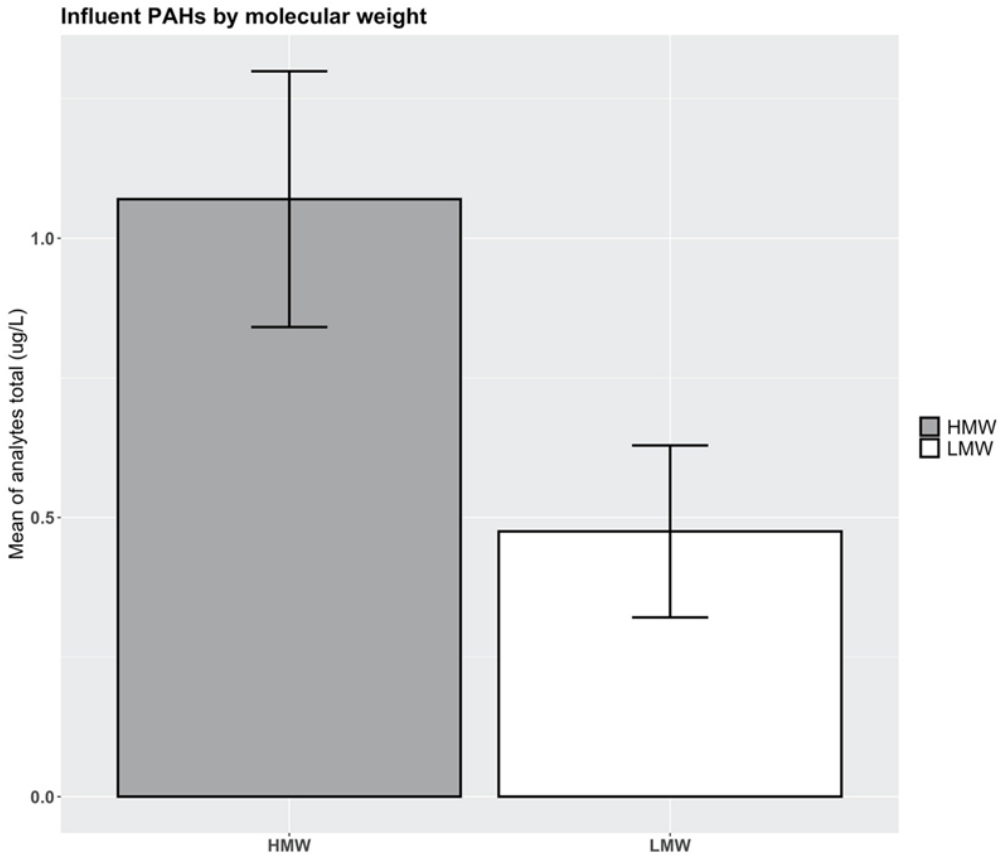

Figure 10. Influent PAH concentrations by molecular weight. High molecular weight (HMW) PAHs have 4-6 rings, and low molecular weight (LMW) PAHs have 2-3 rings. The bars show the mean and standard error bars for the total concentrations across events.

PAH sources in stormwater can be inferred by the relative abundance of high and low-molecular-weight PAH compounds (Brown and Peake 2006). High molecular weight (HMW) PAHs tend to be classified as *pyrogenic*, meaning they were produced via combustion or pyrolysis of organic material. Low molecular weight (LMW) PAHs tend to be classified as *petrogenic*, meaning they originate from fossil fuels and other petroleum products. The stormwater source for this study produced influent enriched in HMW PAHs (Figure 10), suggesting that the bulk of PAH influent loading originated from combustion processes. Since the source of stormwater runoff was from an elevated highway, the HMW PAHs in this study most likely originate from vehicle combustion.

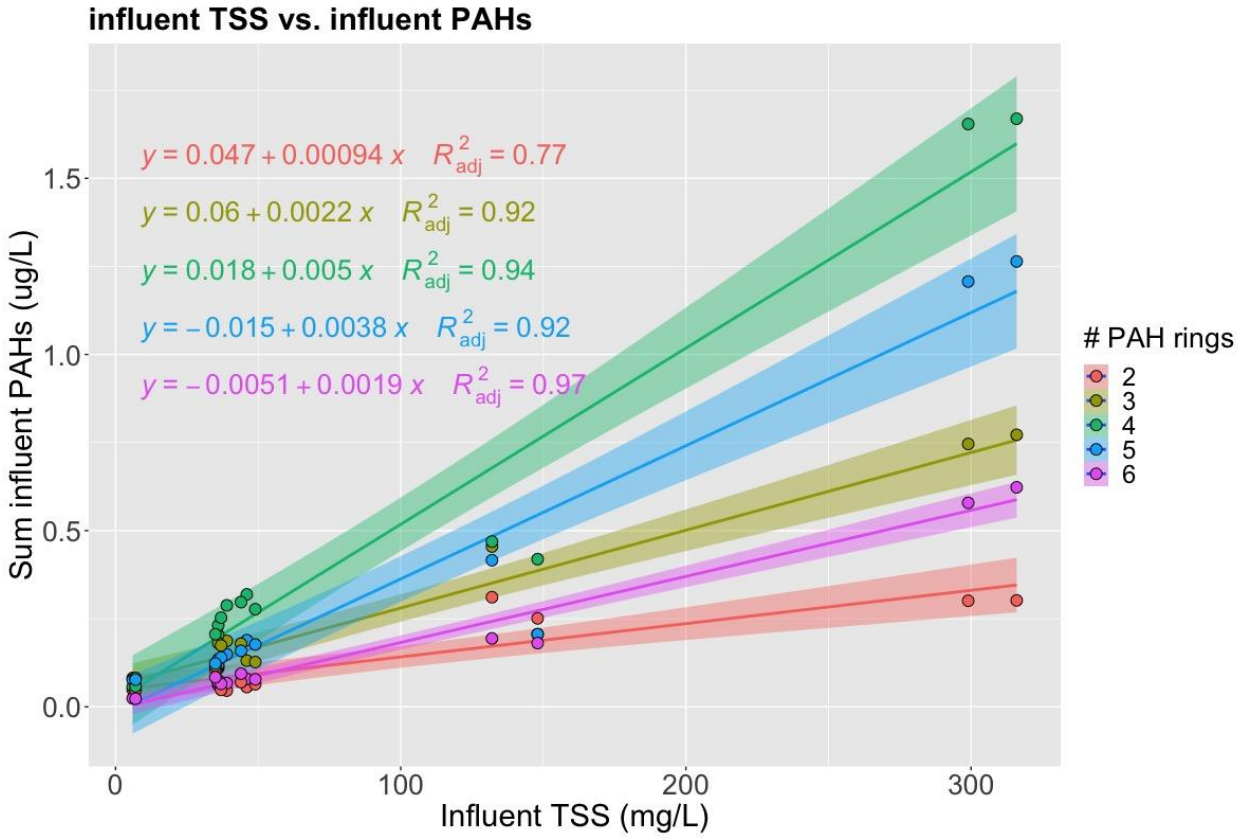

Figure 11. Correlation between influent TSS and PAH analytes classified by PAH ring number. PAH values are the summed mean value by ring number for each sample.

Correlations between PAHs and TSS in stormwater influent can be useful for inferring similarities in TSS and PAH transport since HMW PAHs tend to sorb more readily to particles than LMW PAHs due to their increased hydrophobicity (Nielsen et al., 2015). Our data show that HMW PAHs (4-6 rings) were more strongly correlated with TSS concentrations compared with LMW PAHS (Figure 11). Four ring PAHs (e.g., fluoranthene and pyrene) had a particularly strong, positive correlation with TSS ($R^2 = 0.94$, $p < 0.001$).

Dissolved Organic Carbon (DOC) in the influent ranged from 0.5-31.7 mg/L with a median of 1.6 mg/L and a geomean of 2.54 mg/L. DOC in the field stormwater grab samples ranged from 1.25-26.7 mg/L with a median of 2.63 mg/L and a geomean of 2.96 mg/L. DOC was exported from all bioretention columns. In effluent samples, DOC concentrations had a geomean of 16.1 mg/L, a median of 14.6 mg/L, and a range of 4.78-52.1mg/L. Biochar – amended columns (BSM+ BC and BSM+ BC+ Fungi) exported less DOC than columns without biochar (Figure 12). The only exception to this trend was event 4, the event with the highest influent DOC concentration. Despite effluent DOC concentrations being significantly correlated to influent DOC concentrations, generally, effluent DOC concentrations decreased throughout the study after dosing event 4.

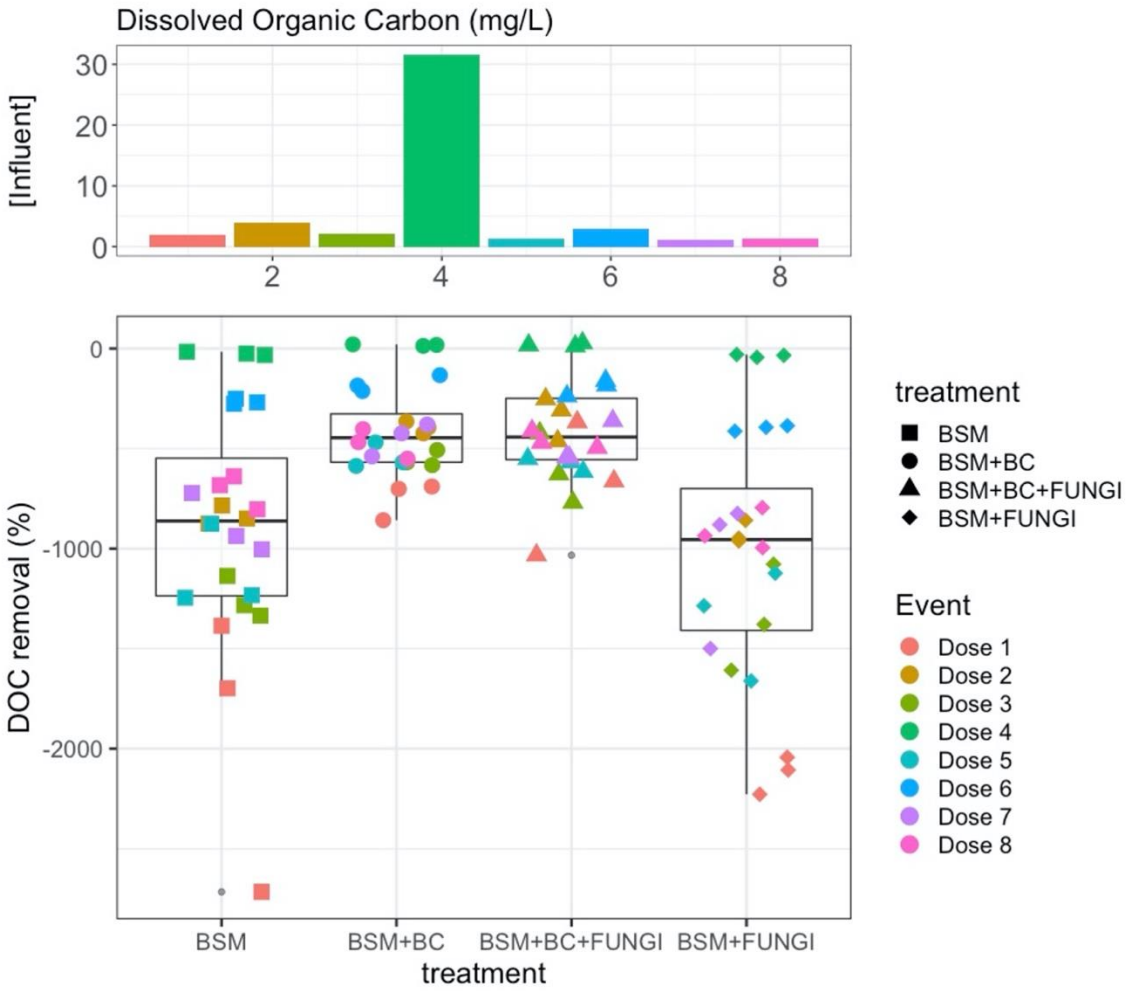

Figure 12. Top) Influent concentrations for each dosing event, and (bottom) corresponding percent removal rates for each treatment pooled across all dosing events. Negative removal values indicate export.

Total Suspended solids in the influent samples ranged from 6 - 316 mg/L with a median of 41.5 mg/L and a geomean of 49.3 mg/L (Figure 13). TSS showed net removal for all events except for events 1 and 5 (2020-02-06 and 2020-10-13, respectively). Event 5 was also the event with the lowest influent TSS concentrations throughout the study. During event 5, all treatments exported TSS, with BSM control exporting the highest TSS concentrations and BSM+BC+FUNGI exporting the lowest TSS concentrations. TSS removal was highest for events with high influent TSS concentrations.

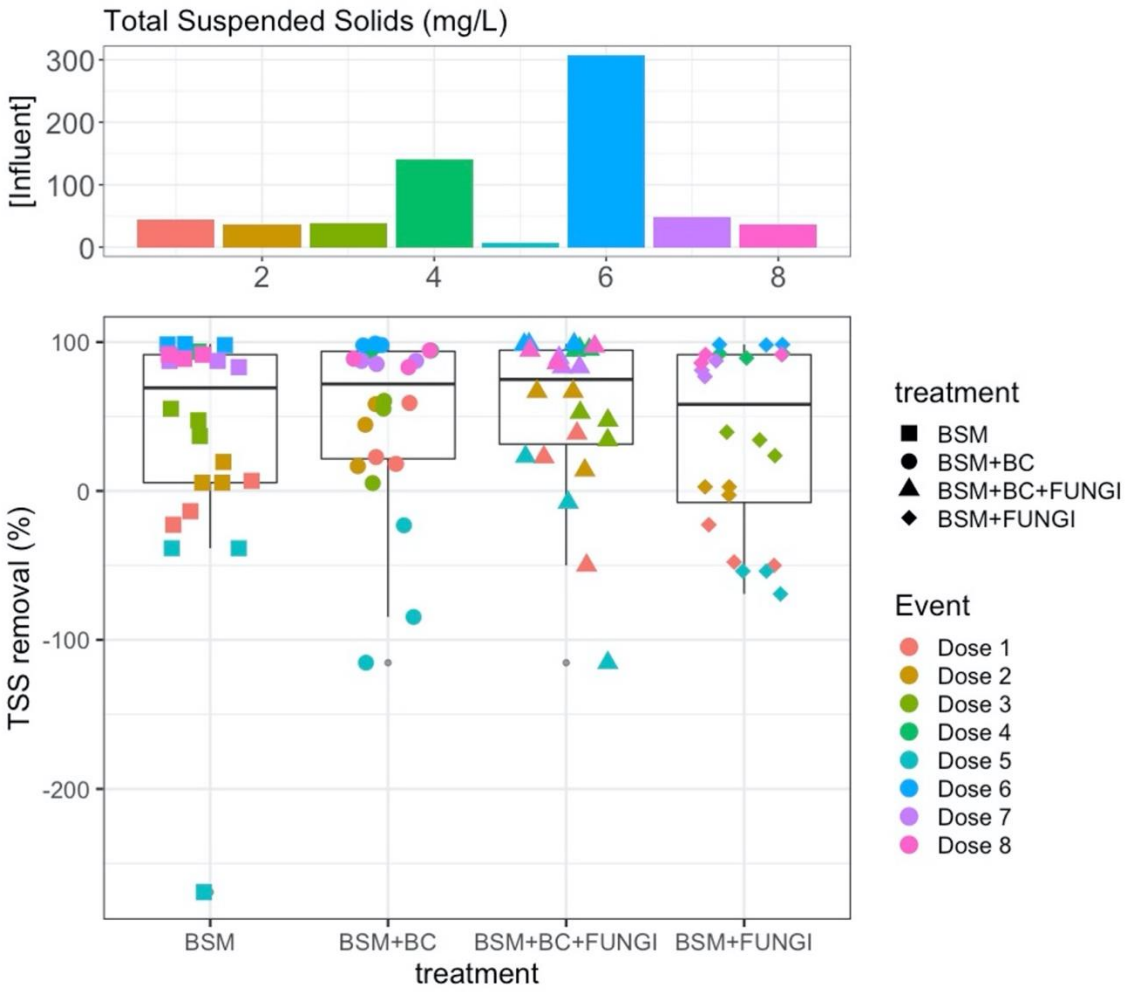

Figure 13. Top) Influent concentrations for each dosing event, and (bottom) corresponding percent removal rates for each treatment pooled across all dosing events. Negative removal values indicate export.

The Washington Department of Ecology has set stormwater BMP performance goals for TSS. Basic treatment of TSS is defined as:

- 80% removal for TSS influent concentrations between 100 – 200 mg/L. For influent concentrations below 100 mg/L, effluent concentration should not exceed 20 mg/L (WDOE 2019).

TSS treatment performance for the dosing events in this study is shown in Figure 14. Performance of the columns, in terms of Ecology's basic criteria, appears to have improved with study age. TSS performance criteria were not met for the conditioning event or dosing event 1, 2, or 3. From dosing event 4 through the end of the study criteria were met by most samples with the exception of 2 samples during dose event 5 (Figure 14).

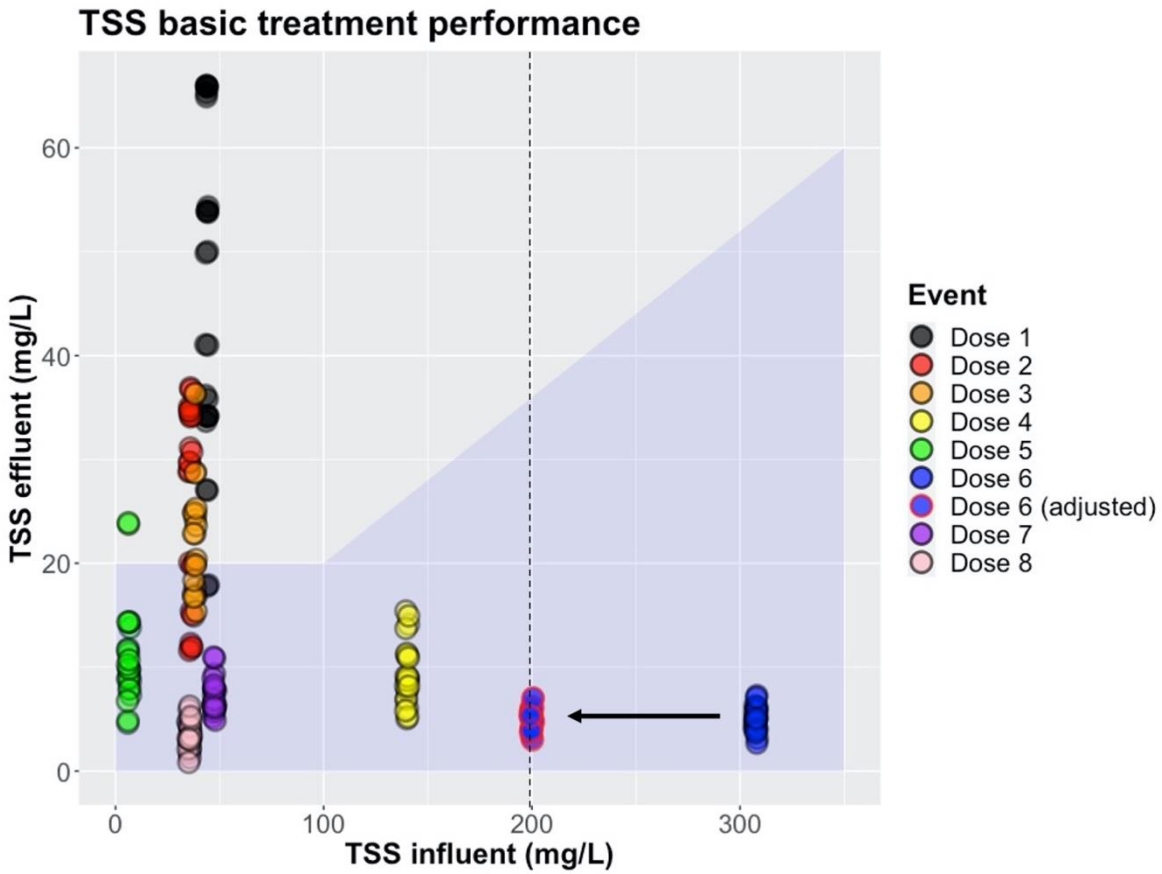

Figure 14. Treatment performance of TSS in bioretention columns by dosing event. The blue shaded region represents the data region that meets W.A.'s basic treatment criteria for TSS treatment in stormwater BMPs (described below). The dose 6 (adjusted) points show dose 6 data with the influent value replaced with 200 mg/L per Ecology's basic treatment guidelines.

4.2.3 Random intercept model results

Linear mixed effects models (with dosing event as a random intercept) were fit to removal data for each of the target contaminants. Removal rates for *E. coli*, Fecal coliform, DOC, and TSS were calculated as log removal (*log[influent/effluent]*) to meet the assumption of normality. PAH removal was not modeled because nearly all effluent values were non-detect.

Log *E. coli* removal was significantly higher than the BSM control in the biochar-amended treatments, BSM+BC (t-stat = 3.02, p = 0.003) and BSM+BC+FUNGI (t-stat = 2.37, p = 0.02) (Table 6). The beta coefficients for biochar-amended treatments were positive, indicating significantly greater log *E. coli* removal in these treatments compared with the control BSM treatment. The variance partitioning coefficient, ρ, of event in the log *E. coli* removal model was 0.425, indicating that 42.5% of the unexplained variability in log *E. coli* removal (after controlling for treatment) is attributable to dosing event (Table 7).

Log Fecal Coliform removal was significantly higher than the BSM control in the BSM+BC+FUNGI treatment (t-stat = 2.9, p = 0.005). The beta coefficients for the biochar and

fungi amended treatment was positive, indicating significantly greater log *E. coli* removal in this treatment compared with the control BSM treatment. For this model $\rho = 0.354$, indicating that 35.4% of the unexplained variability in log Fecal coliform removal (after controlling for treatment) is attributable to dosing event (Table 7).

Log DOC removal was significantly higher in the biochar-amended treatments, BSM+BC (t-stat = 11.08, $p < 0.001$) and BSM+BC+FUNGI (t-stat = 11.27, $p < 0.001$) than the BSM control. The beta coefficients for biochar-amended treatments were positive, indicating greater log DOC removal in these treatments compared with the BSM control. The BSM+FUNGI treatment had a significant negative coefficient, indicating lower log DOC removal in this treatment compared with the control. The intercept was also significant in this model (t-stat = -7.05, $p < 0.001$), suggesting that the mean log DOC removal value is not 0. For this model $\rho = 0.821$, indicating that the majority (82.1%) of the unexplained variability in log DOC removal is attributable to dosing event (Table 7).

Log TSS removal in the BSM+BC+FUNGI was significantly higher than the BSM control treatment (t-stat = 2.97, $p = 0.004$). The intercept was also significant in this model (t-stat = 2.45, $p = 0.044$), suggesting that the mean log TSS removal value is different from 0. For this model $\rho = 0.830$, indicating that the majority (83%) of the unexplained variability in log TSS removal is attributable to dosing event (Table 7).

Table 6. Statistical summary of random intercept mixed effects models. Parameter estimates (coefficients, standard error, t-statistics, degrees of freedom, and p-values) are provided for fixed effects. Standard deviations are provided for random effects. Bolded p-values indicate significance at the $\alpha = 0.05$ level.

Model	**Effect**	**Group**	**Term**	**Estimate**	**S.E.**	**t-statistic**	**df**	**p-value**
log EC removal	fixed		(Intercept)	0.163	0.677	0.24	11	0.814
	fixed		BSM+BC	1.781	0.589	3.02	73	0.003
	fixed		BSM+BC+FUNGI	1.398	0.589	2.37	73	0.02
	fixed		BSM+FUNGI	0.764	0.596	1.28	73	0.204
	random	Event	Std. dev (Intercept)	1.412				
	random	Residual	Std. dev Observation	1.907				
log FC removal	fixed		(Intercept)	0.755	0.639	1.18	16	0.255
	fixed		BSM+BC	0.903	0.656	1.38	71	0.173
	fixed		BSM+BC+FUNGI	1.903	0.656	2.9	71	0.005
	fixed		BSM+FUNGI	0.416	0.675	0.62	71	0.54
	random	Event	Std. dev (Intercept)	1.148				
	random	Residual	Std. dev Observation	2.098				
log DOC removal	fixed		(Intercept)	-2.023	0.285	-7.09	7	<0.001
	fixed		BSM+BC	0.559	0.05	11.08	85	<0.001
	fixed		BSM+BC+FUNGI	0.568	0.05	11.27	85	<0.001
	fixed		BSM+FUNGI	-0.152	0.05	-3.02	85	0.003
	random	Event	Std. dev (Intercept)	0.801				
	random	Residual	Std. dev Observation	0.175				

Model	Effect	Group	Term	Estimate	S.E.	t-statistic	df	p-value
log TSS removal	fixed		(Intercept)	1.385	0.566	2.45	7	0.044
	fixed		BSM+BC	0.172	0.094	1.83	85	0.071
	fixed		BSM+BC+FUNGI	0.279	0.094	2.97	85	0.004
	fixed		BSM+FUNGI	-0.118	0.094	-1.25	85	0.213
	random	Event	Std. dev (Intercept)	1.591				
	random	Residual	Std. dev Observation	0.325				

Table 7. Variance partitioning for random intercept models. Level 1 variability is the unexplained variance in the fixed effects after controlling for treatment. Level 2 variability is the unexplained variance in the random effects (event) after controlling for treatment. Total variability is the sum of Level 1 and Level 2 variability. The variance partitioning coefficient, ρ, is the proportion of total variability made up by Level 2 (*Level 2 variability/Total variability*). Higher values of ρ indicate greater clustering of response variable values by dosing event.

Model	Level 1 (residual)	Level 2 (Event)	Total	Variance partitioning coefficient, ρ
log EC removal	1.907	1.412	3.319	0.425
log FC removal	2.098	1.148	3.246	0.354
log DOC removal	0.175	0.801	0.976	0.821
log TSS removal	0.325	1.591	1.916	0.830

4.3 Transport of bacteria by TSS

When bacteria (Fecal coliform or *E. coli*) were measured in the effluent samples (effluent concentrations > detection limits) across all columns and all events, we observed a significant, positive correlation between TSS and bacteria counts in effluent samples (TSS vs Fecal coliform in Figure 15; TSS vs *E. coli* in Figure 16). Pearson correlation coefficients for the relationships between natural log-transformed TSS (ln(TSS)) and ln(Fecal coliform) and ln(*E. coli*) were 0.83 ($p < 0.001$) and 0.6 ($p < 0.001$), respectively. The more general enumeration of bacteria expressed by Fecal coliform yielded a higher correlation with particulate matter (TSS) when compared with *E. coli.*

When Fecal coliform export was observed in some samples, the majority of those samples were associated with higher TSS measurements – see points colored in red in Figure 15. Export of Fecal coliform was also associated with a few mid-range TSS values. Despite a weaker correlation between TSS and *E. coli*, export of *E. coli* from the columns were also associated with mid to high TSS measurements in the effluent (red points in Figure 16)

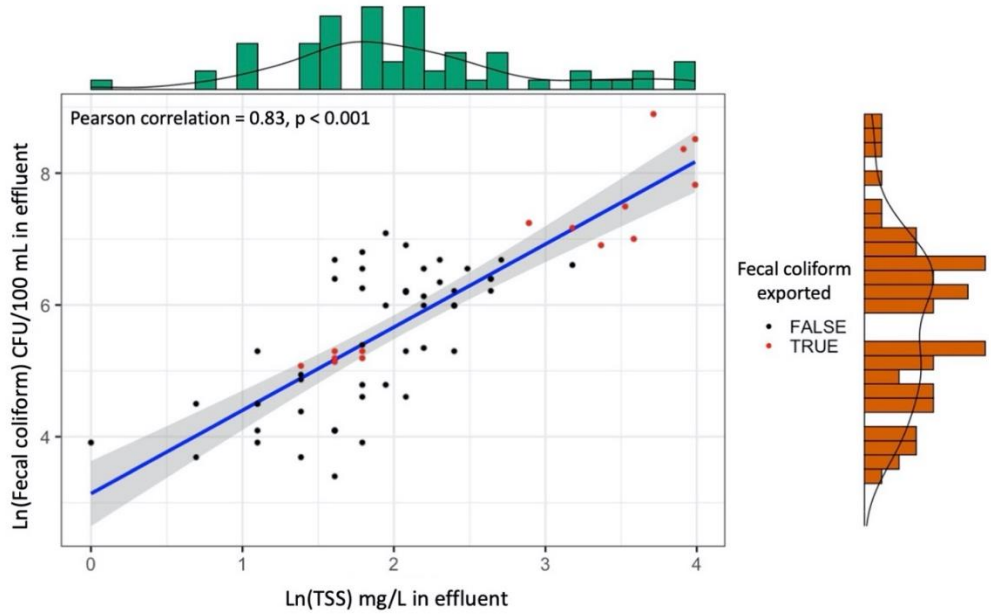

Figure 15. Scatterplot representing the correlation between natural log-transformed TSS and natural log-transformed Fecal coliform in effluent samples. Samples with non-detects for Fecal coliform were omitted. Points labeled in red indicate effluent Fecal coliform concentrations were greater than influent concentrations (Fecal coliform export).

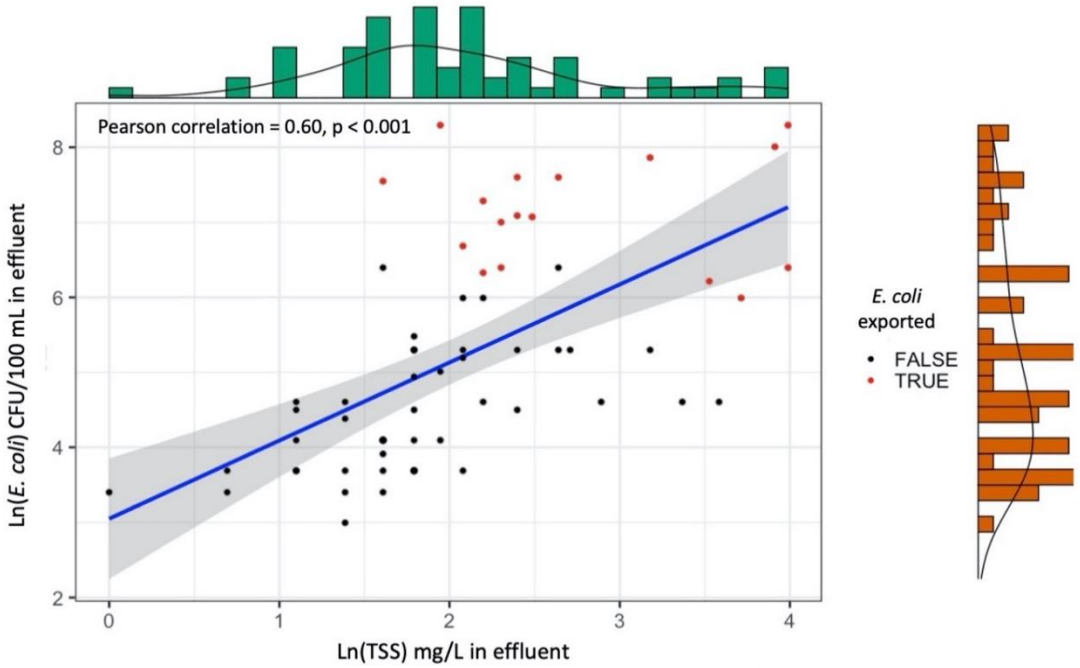

Figure 16. Scatterplot representing the correlation between natural log-transformed TSS and natural log-transformed *E. coli* in effluent samples. Samples with non-detects for *E. coli* were omitted. Points labeled in red indicate effluent *E. coli* concentrations were greater than influent concentrations (*E. coli* export).

4.4 PAHs in bioretention soils

Each bioretention column's soil matrix was sampled for PAHs during four soil sampling events throughout the study. The first soil samples were taken directly following the initial column conditioning to establish "baseline" PAH concentrations in the media before dosing with stormwater. Samples were taken from 2 depths during each sampling event: 6 inches and 11inches from the media surface. After 2 soil sampling events, it appeared that stormwater dosing was not increasing soil PAH concentrations at the two sampled strata. To check whether PAH accumulation due to stormwater input was not confined to the soil surface alone, surface samples were taken from 1 column of each treatment type (shown as red points in Figure 17) during the 3rd soil sampling event. No difference in PAH concentrations was observed amongst the various depths sampled (Figure 17), so stratum was not considered a model factor, and data from each stratum were pooled for each column to increase statistical power. This resulted in 2 data points per column per sampling event, totaling 6 data points per treatment for each event.

PAH concentrations generally decreased throughout the study, despite inputs from stormwater dosing. Temporal trends in PAH concentrations differed across PAH analytes, with 3-ring and 4-ring PAHs showing clear decay patterns over time (Figure 18). Five and 6 ring PAHs (High Molecular Weight), except for chrysene, did not show marked decreases in concentration over time. Two-ring PAHs showed some decrease over time, but their decay was minimal compared to 3 and 4 ring compounds.

We expected to find high PAH concentrations in shallow column depths because others have reported that PAHs in bioretention soils are most dominant closer to the soil surface (Diblasi et al., 2009). Even when we sampled the surface layer in all the columns to see if we were missing the depth where PAHs in the influent stormwater might be adsorbed, we did not see any notable increase in the concentrations for surface samples compared with the two lower sampled strata. This lack of stratification of PAH concentrations supports the hypothesis that most measured PAHs originate from the media itself and not from stormwater inputs. Mass balance calculations in the next section further support this hypothesis.

PAH movement and breakdown in soils are thought to be driven by molecular weight/ring number/size (Kanalay and Harayama 2000). Low molecular weight (LMW) PAHs (2-3 rings) are thought to be more soluble in water than high molecular weight (HMW) PAHs, allowing them to be transported more easily in water. Also, LMW-PAHs are less likely to sorb to media (Nielsen et al., 2015), further lending them to loss via effluent transport. Finally, four-ring PAHs fall into the HMW category and are typically considered to be hard for microbes to break down (Kanalay and Harayama 2000). Given these differences between LMW and HMW PAHs, we expected to see most PAH loss in the soil media over time to be dominated by LMW PAH compounds loss – where the loss was directly measured in the effluent or inferred indirectly by doing a mass balance analysis and accounting for inputs, storage, and loss terms. However, we saw that 3 and 4 ring PAHs were the greatest species of TPAHs that were lost over time. It is possible that the initial dominance of 3 and 4 ring PAHs in the media primed the microbial community to use these PAHs as a food source, allowing for more rapid degradation of these compounds and therefore measured as loss.

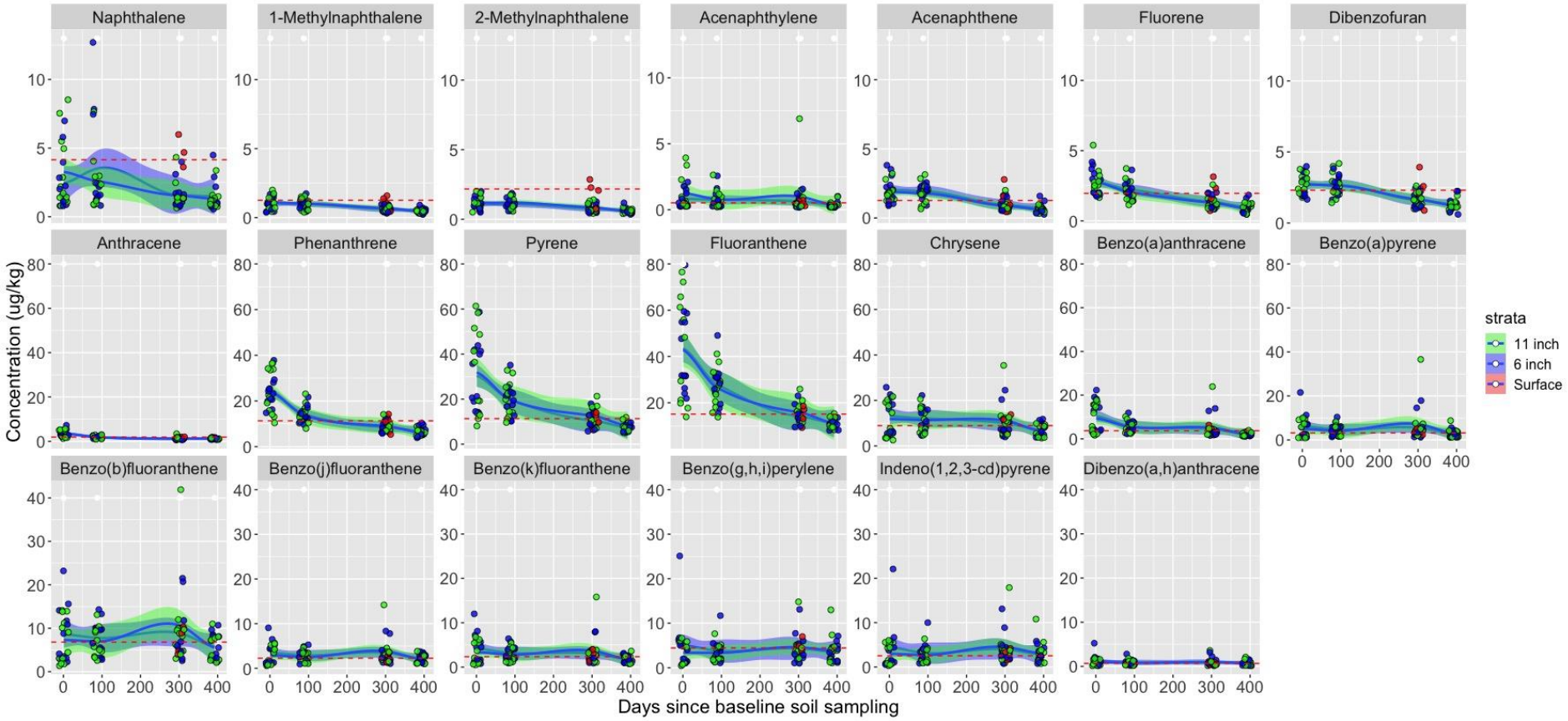

Figure 17. Soil PAH analyte concentrations (ug/kg) by sampling depth. Compounds are shown in order (left → right) of low to high molecular weight. Surface samples were taken from the surface of a subset of bioretention columns on the third soil sampling data in order to capture PAHs retained within 2 cm of the media surface. Median surface PAH values are shown as a horizontal red dashed line. Loess lines show local polynomial regression fitting corresponding 95% confidence intervals. Y-axes differ across rows.

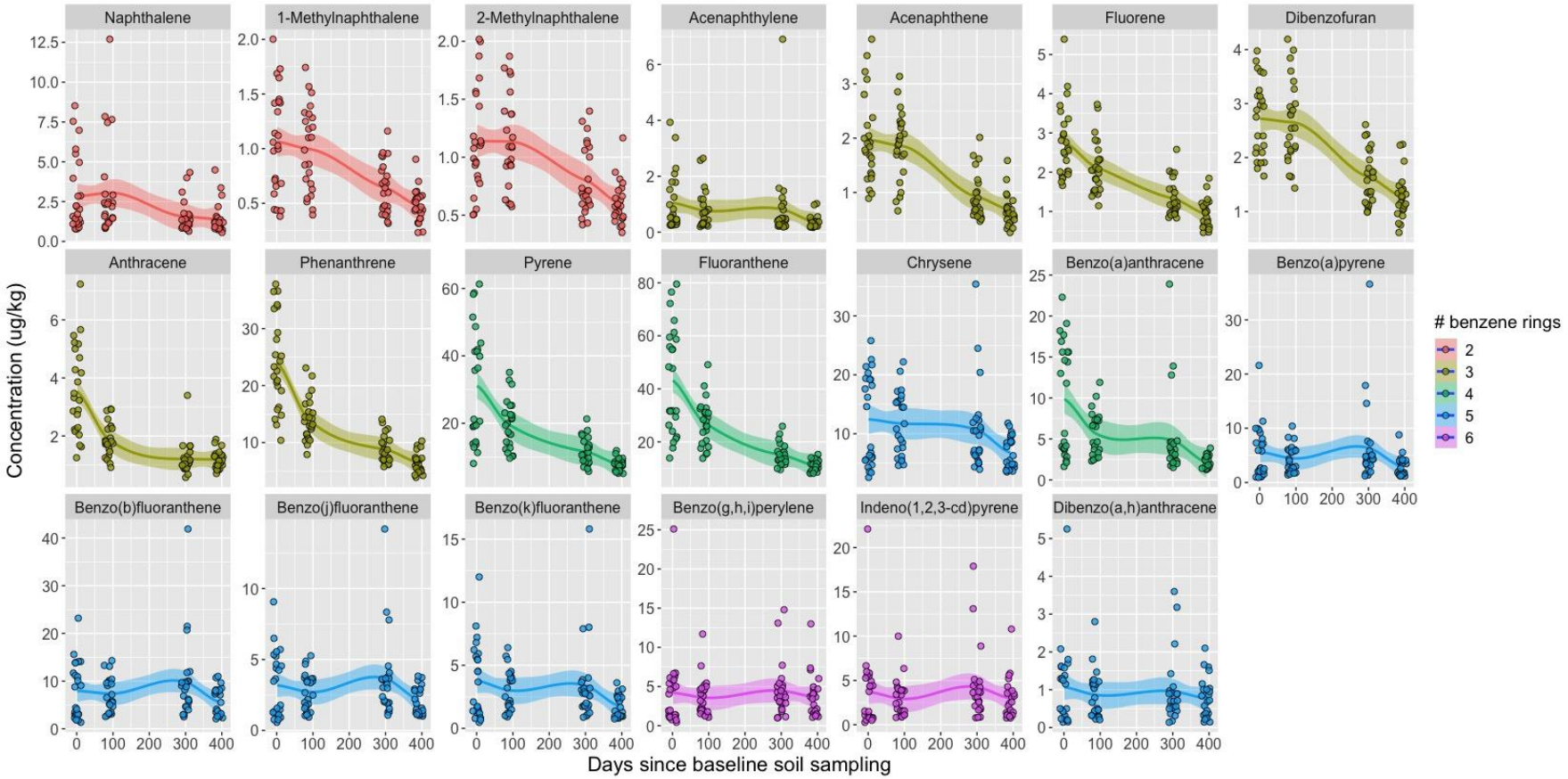

Figure 18. Soil PAH analyte concentrations (ug/kg) by the number of rings in the PAH compound. Loess lines show local polynomial regression fitting corresponding 95% confidence intervals. Surface samples were omitted from this figure. Y-axes differ by analytes to allow Visualization of time trends. Plots are arranged from upper left to lower right by increasing molecular weight. Colors denote number of rings.

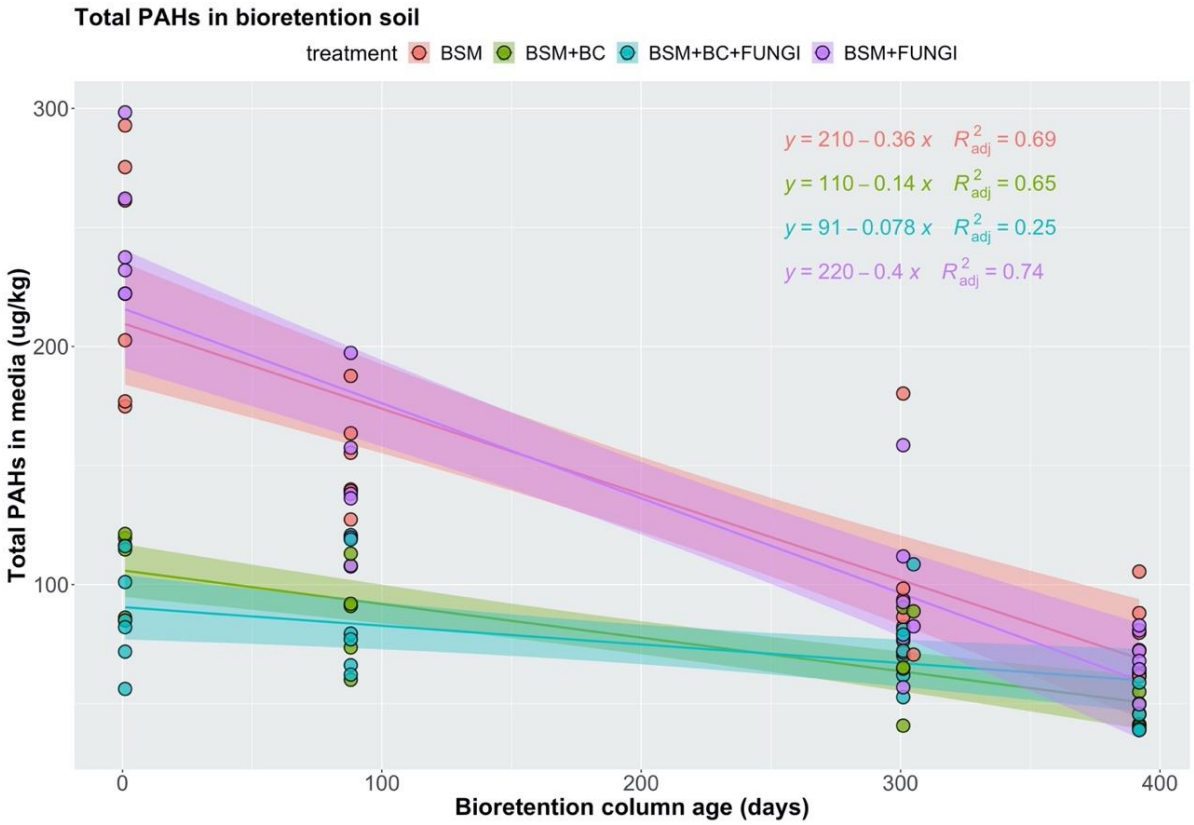

Figure 19. Total PAHs in bioretention soil samples across 4 soil sampling events.

Bioretention soils that were not amended with biochar (BSM control, BSM+ fungi) initially contained higher total PAHs concentrations than biochar-amended soils (BSM+BC, BSM+BC+ fungi). Over time, Total PAHs in the BSM control and BSM+ fungi treatments decreased, converging to similar concentrations as the BSM+BC and BSM+BC+ fungi treatments.

These results suggest that the initially observed differences in Total PAH concentrations were likely caused by the partial replacement of compost with biochar in the two mixes with lower Total PAH concentrations. The biochar-amended mixes comprised 60% sand, 20% compost, and 20% biochar (by volume), while the unamended mixes comprised 60% sand and 40% compost (by volume). Therefore, it is highly probable that the compost is a source of PAHs, and that replacing some compost with biochar results in lower soil Total PAHs due to the reduced overall abundance of compost.

4.4.1 TPAH Mass balance analyses

A mass balance conducted of TPAH in each bioretention column based on soil samples and TPAH inputs and exports during dosing experiments showed that the highest initial TPAH masses were measured in the BSM+ FUNGI columns (Table 8), and the lowest in the BSM+BC+ FUNGI columns. Columns that did not receive a 50% (v/v) replacement of compost with biochar (BSM control, and BSM+ FUNGI) started with more than twice the mass of

TPAHs as the columns amended with biochar (BSM+BC and BSM+BC+FUNGI). This result further added validation to the previously stated idea that compost in BSM is a source of TPAHs. The BSM control columns also exported the most TPAHs throughout the study. However, and importantly, it should be noted that the export (in the effluent) of TPAHs from BSM (control) columns was minimal compared to the mass of TPAHs in the soil media and the stormwater inputs (Table 8).

TPAH masses in BSM control and BSM+FUNGI columns changed the most between initial and final soil sampling compared with the two biochar-amended treatments (Table 8). The BSM control and BSM+FUNGI treatments exported low mean TPAH masses (32.6 µg and 1.1 µg, respectively) via effluent over the 6 events. However, not as low as the biochar-amended columns (BSM+BC and BSM+BC+FUNGI) which consistently yielded non-detect values for all effluent data. The highest mean TPAH export amongst all the treatments were associated with the BSM control (32.6 µg), but this higher export mass appeared to be driven by PAH breakthrough from one BSM control column (Column 10), which had a total export of 95.1 µg (mean effluent mass over the six storms), compared to mean export values of just 1.4 µg and 1.3 µg from the other two BSM control columns.

Based only on the total mass of TPAHs entering the columns via stormwater dosing (mean of 448 µg), each column's initial soil TPAH mass, and TPAH lost via effluent (Table 8); we should have seen an increase in each column's soil TPAHs by an average of 3% for the BSM control, 2.9% for BSM+FUNGI, 6.8% for BSM+BC, and 8.4% for BSM+BC+FUNGI . However, a consistent net loss of soil TPAH mass was observed in the bioretention media over the period of study. The net loss of TPAHs from the bioretention soil was likely driven by some internal loss mechanism, such as bioremediation, plant uptake, or volatilization. Other studies of PAH fate in bioretention cells have found that PAH loss through volatilization is an insignificant loss mechanism compared with mineralization (i.e., complete biodegradation) and plant uptake (Lefevre 2012a). For PAH volatilization to occur, there needs to be an air-water interface for the PAHs to pass through. In a bioretention system, the most extensive air-water interface exists during ponding. PAH uptake by plants was not measured as it was out of the scope of this study.

Table 8. Mass balance of Total PAHs (TPAHs) during the study period from the first soil sampling event on 12/13/2019 to the last soil sampling event on 01/07/2021. PAH input and export from dosing events 7 and 8 were not included in the mass balance because they took place after the final soil sampling event. Data from the two soil sampling strata (Figure 4) were averaged because it was determined that there was no difference in total PAHs between the two strata (see Figure 16). Mass balance calculations were performed on each column's data and then averaged by treatment, resulting in per column means and standard errors (s.e.) grouped by treatment with n=3.

All units in µg or %	**Initial (soil)**	**Input (via influent)**	**Export (via effluent)**	**Net (soil)**	**Expected change in soil TPAH**	**End (soil)**	**Measured change in soil TPAH**	
Per column metrics	Mean (s.e.)	Mean	Mean (s.e.)	Mean	%	Mean (s.e.)	Mean	%
BSM control	14,870 (2,160)	448	32.6 (31.3)	416	3.0	5,023 (347)	-9,847	-65.3%
BSM+BC	6,800 (738)	448	0 (0)	448	6.8	2,883 (223)	-3,917	-56.8%
BSM+FUNGI	15,336 (854)	448	1.1 (0.6)	447	2.9	4,347 (221)	-10,989	-71.6%
BSM+BC+FUNGI	5,434 (467)	448	0 (0)	448	8.4	3,272 (351)	-2,162	-38.0%

- The **Initial** mass is the baseline soil TPAH concentration * media mass for each column.
- **Input** is the sum of influent TPAH mass (TPAH concentration * 54 L of influent) across six events.
- **Export** is the sum of effluent TPAH mass (TPAH concentration * 54 L of effluent) per column across six events.
- **Net** is calculated by Input – Export.
- **Expected change in soil TPAH** is the expected percent increase in soil TPAH mass per column (averaged by treatment) based on the sum of initial TPAH and Net TPAH.
- **End** mass is the final soil TPAH concentration * media mass for each column.
- **Measured change in soil TPAH** is the absolute and percentage change in TPAH mass in the soils based on the difference between the initial and final mass of soil TPAHs .

4.4.2 Plant data

Plant biomass and root length were recorded while planting the columns, but columns were left intact at the end of the study so there is no data for change over time for these measurements. Plant height, maximum width, and base width were measured for each plant during 3 points in the study to determine if column media had any effect on plant growth. These plant metrics were used to estimate the volume of the plant (Figure A3). A single-factor one-way ANOVA was run to test for the effect of column media on the change in plant above-ground biomass volume between the first and last measurements. The ANOVA suggested no significant effect of column media on plant growth (F-stat = 0.06, p-value: 0.98). With no statistical difference between the growth of plants by bioretention mix, plant data were not used further to help explain pollutant removal efficiencies by the columns.

5 Discussion and recommendations

5.1 Stormwater treatment

5.1.1 Bacteria

E. coli and Fecal Coliform were initially exported from some columns, but removal performance appeared to improve over time. Biochar-amended columns removed significantly more *E. coli* than control BSM columns. Columns amended with both biochar and fungi removed significantly more Fecal coliform than BSM control columns. Understanding the treatment effects on Fecal coliform is less clear because the individual biochar (BSM+BC) and fungi (BSM+FUNGI) amendments did not show significant impacts on removal. However, both the BSM+BC and BSM+FUNGI treatments had positive beta coefficients, indicating there may be a slightly positive impact of both these amendments on Fecal coliform removal that is only significant when the amendments are used together. Bacteria concentrations in effluent samples were positively correlated with the concentrations of TSS in the effluent. These results suggest that bacteria export from the columns were likely being transported via attachment to particles.

Spromberg et al. (2016) and McIntyre et al. (2020) used similar methods and stormwater sources as the present study, making them useful for contextualizing our bacteria results. Spromberg et al. (2016) used runoff from an elevated arterial road in Seattle, WA to dose bioretention columns. McIntyre et al. (2020) sourced runoff from an urban catchment under the Ship Canal Bridge on I-5. McIntyre et al. (2020) sampled influents and effluents from 12 bioretention columns for 2 years over 8 storm events. Spromberg et al. (2016) sampled 4 replicate columns during 2 events and pooled effluent samples.

Figure 20 compares influent and effluent mean or median concentrations of E. coli and Fecal coliform from this study to similar studies. Influent *E. coli* concentrations for this study (mean = 485 CFU/100 mL); Fecal coliform: mean = 1,268 CFU/100 mL) were mostly within the range of values reported by Spromberg et al. (*E. coli* median = 355 CFU/100 mL; Fecal coliform median = 560 CFU/100 mL) but were in the lower range of mean values reported by McIntyre et al. (*E. coli*:1- 4,867 CFU/100 mL, Fecal coliform: 113-5,500 MPN/100 mL). The present study's fecal coliform influent data were lower on average than the stormwater monitoring data presented in Hobbs et al. (2015).

The present study suggests that bacterial removal was lower than treatment by mesocosms in McIntyre et al. (2020), but similar to limited data available for Spromberg et al. (2016). On average, effluent *E. coli* and Fecal Coliform concentrations were similar across these studies; however, maximum bacteria concentrations were higher in the effluents of this study than for the summary data available for Spromberg et al. (2016) or McIntyre et al. (2020). Samples from the present study appear to show export more often than the other studies, though maximum effluent values were not available for McIntyre et al. (2020). McIntyre et al. (2020) utilized outdoor mesocosms much larger than the greenhouse columns used in the present study. They also received stormwater whenever a storm occurred, while the greenhouse columns only received stormwater during experimental dosing events. These environmental differences may explain some of the disparity between study results.

Cases of FIB export from bioretention columns raise questions around the sources, fate, and transport of bacteria measured in influent and effluent samples. Because the stormwater runoff used in this study was collected from an elevated highway, the potential fecal sources in the contributing catchment are limited to bird waste and any trace sources transported onto the roadway by vehicles. Despite the limited potential for fecal contamination of this catchment, we observed influent Fecal coliform concentrations as high as 4,200 CFU/100 mL, and *E. coli* concentrations as high as 1,300 CFU/100 mL. This suggests that bacteria of non-fecal origin may be triggering false positives in the membrane filtration enumeration. False positives from this method have been documented in surface water samples (Caplenas and Kanarek 1984, McClain et al. 2011, Taylor et al. 2015). Spromberg et al. (2016) also used influent from an elevated highway, which may explain why influent FIB values for the present study are more similar to Spromberg et al.'s results than to results from McIntyre et al. 2020, which used runoff from a more complex urban catchment.

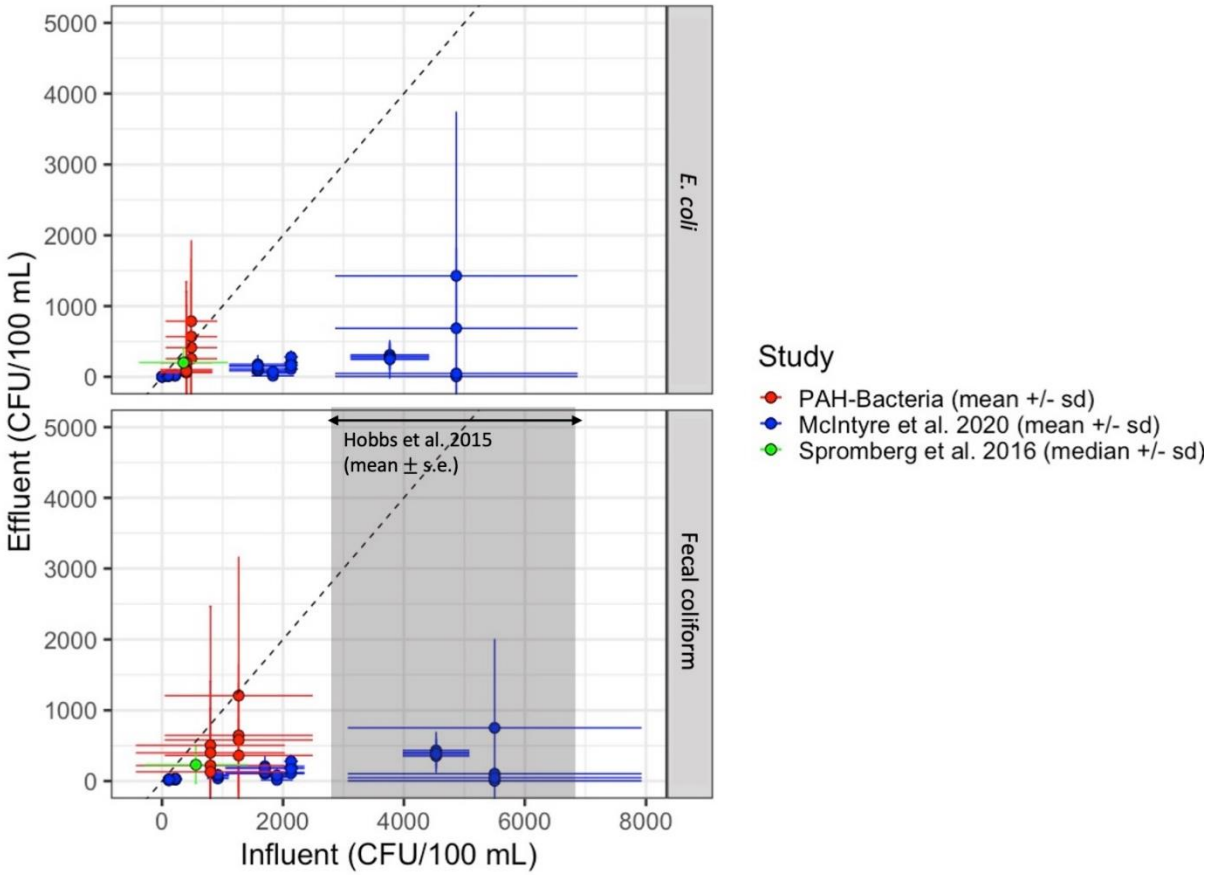

Figure 20. Influent vs. effluent mean, median, and maximum concentrations (CFU/100 mL) of *E. coli* and Fecal Coliform reported in Spromberg et al. (2016), McIntyre et al. (2016), and the present study. Error bars represent ± one standard deviation.

5.1.2 PAHs

Influent total PAH concentrations ranged from 0.089-4.62 ug/L with a geomean of 0.66 ug/L. The most abundant PAHs in influent samples were pyrene (15.2%), fluoranthene (13.1%), and phenanthrene (9.1%). Most PAH influent concentrations were within the lower end of the ranges reported for Western Washington by Hobbs et al. 2015 (Table 6).

PAH removal was > 97% for 94 of 96 effluent samples analyzed in this study. The majority of PAHs in effluent samples were below the analyte detection limits, with only 7 samples having detectable concentrations of PAHs – 3 samples from the BSM control, 3 samples from BSM+FUNGI, and 1 sample from BSM+BC. Since non-detects dominated effluent data, it was not possible to discern any treatment effects for PAH removal.

The relatively low influent PAH concentrations reported here may have led to the near-complete TPAH removal we observed. It is not clear if removal rates would be the same under higher PAH loading rates.

5.1.3 Dissolved Organic Carbon

DOC export was lower in biochar amended treatments than in treatments with the full 40% compost by volume. DOC export is not necessarily a pollution concern, and DOC can be beneficial to aquatic ecosystems. It can form complexes with dissolved metals, providing protection against metal toxicity in fish. For example, McIntyre et al. (2008) found that DOC concentrations > 6 mg/L can eliminate copper olfactory toxicity in coho salmon. We found DOC concentrations ranging from 5-52 mg/L in bioretention column effluents. DOC export may provide additional protection against dissolved metals in systems that have naturally low DOC concentrations.

Though DOC is naturally occurring and can provide some protectiveness against metal toxicity, it can also negatively impact aquatic ecosystems. Excessive DOC can reduce light penetration in water (affecting plant growth), contribute to eutrophication, increase contaminant transport, and cause complications with drinking water treatment (Pagano et al., 2014).

5.2 PAHs in bioretention soil

PAHs are a common and potentially dangerous chemical found in soils. The EPA has established screening levels for PAHs in soils that are protective to various organisms. The most sensitive EPA soil screening level for PAHs is 1.1 mg/L HMW PAHs for mammals. The highest HMW PAH concentration across all samples was 0.262 mg/L, well below the most sensitive screening level.

There was a decrease in soil TPAH concentrations throughout the study for all treatments despite the continuous addition of TPAHs through stormwater, and the removal of TPAHs in the effluent. This result suggests that over time soil TPAH concentrations are being removed through microbial processes or some other form of in-situ TPAH degradation. The fact that soil TPAH concentrations were so much higher in the soil baseline samples suggests that the primary PAH source is from the BSM control itself, specifically the compost, and not from stormwater. This hypothesis is supported by the lower initial TPAH concentrations in the BSM+BC columns,

because the columns containing biochar have half the volume of compost than the columns without biochar.

5.3 Novel amendment evaluation

5.3.1 Biochar

Biochar is produced from organic wastes and is a form of long-term carbon storage. The process of making biochar involves cooking organic materials (such as wood waste, compost, or biosolids) under very low oxygen conditions so that carbon is stored in a stable solid structure rather than being released as CO_2 as it would during combustion or microbial breakdown. Biochar is highly porous and adsorptive, it is capable of high water retention, and it supports plant growth (Mohanty et al. 2018). These qualities make biochar an attractive alternative to compost in bioretention systems, as it may serve the same function as compost without exporting contaminants. Because biochar is recalcitrant to microbial degradation, it is likely to last longer than compost in bioretention systems.

In the present study, we found that biochar amendments increased *E. coli* removal, decreased DOC export, and reduced initial PAH concentrations in the bioretention soil media. Since we used a partial replacement of compost with biochar in this study, it is difficult to discern if these observed benefits are attributable to the addition of biochar or the reduction of compost.

Future research on biochar in bioretention systems should focus on determining the practicality of implementation (cost-benefit analysis) and estimating the direct contribution of biochar to bioretention characteristics such as plant growth, contaminant removal, and adsorption capacity over time. Given that biochar properties vary widely based on feedstock and production processes, different biochars should not be considered equal in terms of their treatment capabilities. Some biochars can contain leachable trace organic contamiants and metals, so to ensure the protectiveness of this material to aquatic organisms, toxicity testing should be conducted on biochar effluents.

5.3.2 Fungi

Our findings suggest that fungi may also offer pollutant reduction benefits as a bioretention amendment. Compared to the control bioretention media (BSM), columns with fungi-amended media (BSM+FUNGI) seemed to experience higher rates of PAH loss over the course of the study. Several studies have demonstrated the ability of fungi to improve PAH breakdown in contamianted soils (El Amrani et al. 2015, Haritash and Kaushik 2009). Since fungi are generalist bioremediators who can breakdown a wide range of organic contamiants with extracellular enzymes, they may be especially beneficial for enhancing bioremediation in bioretention systems which receive complex mixtures of PAHs via stormwater.

Though the *Stropharia rugosoannulata* used in the present study was present in inoculated columns throughout the study period, their mycelial networks only appeared to be actively growing during the 2-3 months following inoculation. Future studies should consider the habitat required for sustained fungal growth in bioretention systems, and conduct field scale experiments.

6 References

Abdel-Shafy, H. I., & Mansour, M. S. (2016). A review on polycyclic aromatic hydrocarbons: source, environmental impact, effect on human health and remediation. *Egyptian Journal of Petroleum*, *25*(1), 107–123.

Andersson, J. T., & Achten, C. (2015). Time to Say Goodbye to the 16 EPA PAHs? Toward an Up-to-Date Use of PACs for Environmental Purposes. *Polycyclic Aromatic Compounds*, *35*(2–4), 330–354. https://doi.org/10.1080/10406638.2014.991042

Arnone, R. D., & Perdek Walling, J. (2007). Waterborne pathogens in urban watersheds. *Journal of Water and Health*, *5*(1), 149–162.

Bannerman, R. T., Owens, D. W., Dodds, R. B., & Hornewer, N. J. (1993). Sources of pollutants in Wisconsin stormwater. *Water Science and Technology*, *28*(3–5), 241–259.

Benham, B. L., Baffaut, C., Zeckoski, R. W., Mankin, K. R., Pachepsky, Y. A., Sadeghi, A., … Habersack, M. (2006). Modeling bacteria fate and transport in watersheds to support TMDLs. *Transactions of the ASABE*, *49*(4), 987–1002.

Boving, T. B., & Neary, K. (2007). Attenuation of polycyclic aromatic hydrocarbons from urban stormwater runoff by wood filters. *Journal of Contaminant Hydrology*, *91*(1–2), 43–57.

Brown, J. N., & Peake, B. M. (2006). Sources of heavy metals and polycyclic aromatic hydrocarbons in urban stormwater runoff. *Science of the Total Environment*, *359*(1–3), 145–155.

Caplenas, N.R. and Kanarek, M.S., 1984. Thermotolerant non-fecal source Klebsiella pneumoniae: validity of the fecal coliform test in recreational waters. *American Journal of Public Health*, *74*(11), pp.1273-1275.

Chandrasena, G.I., Pham, T., Payne, E.G., Deletic, A. and McCarthy, D.T., 2014. E. coli removal in laboratory scale stormwater biofilters: Influence of vegetation and submerged zone. *Journal of Hydrology*, *519*, pp.814-822.Ceustermans, A. et al., 2007. Inactivation of Salmonella Senftenberg strain W 775 during composting of biowastes and garden wastes. *Journal of applied microbiology*, Volume 103, pp. 53-64.

Cheng, R. (2017). qtlmt: Tools for Mapping Multiple Complex Traits. R package version 0.1-6. https://CRAN.R-project.org/package=qtlmt.

DiBlasi, C. J., Li, H., Davis, A. P., & Ghosh, U. (2008). Removal and fate of polycyclic aromatic hydrocarbon pollutants in an urban stormwater bioretention facility. *Environmental Science & Technology*, *43*(2), 494–502.

El Amrani, A., Dumas, A.-S., Wick, L. Y., Yergeau, E., & Berthomé, R. (2015). "Omics" insights into PAH degradation toward improved green remediation biotechnologies. *Environmental Science & Technology*, *49*(19), 11281–11291.

EPA, U. S., (2018). Ecological Soil Screening Level (Eco-SSL) Guidance and Documents. U.S. Environmental Protection Agency. https://www.epa.gov/sites/production/files/2015-09/documents/eco-ssl_pah.pdf.

Feist, B.E., Buhle, E.R., Baldwin, D.H., Spromberg, J.A., Damm, S.E., Davis, J.W. and Scholz, N.L., 2017. Roads to ruin: conservation threats to a sentinel species across an urban gradient. *Ecological applications*, *27*(8), pp.2382-2396.

Fox, J & Weisberg, S. (2019). An {R} Companion to Applied Regression, Third Edition. Thousand Oaks CA: Sage. URL: https://socialsciences.mcmaster.ca/jfox/Books/Companion/

Haritash, A. K., & Kaushik, C. P. (2009). Biodegradation aspects of polycyclic aromatic hydrocarbons (PAHs): a review. *Journal of Hazardous Materials*, *169*(1–3), 1–15.

Hobbs, W., B. Lubliner, N. Kale, and E. Newell. 2015. Western Washington NPDES Phase 1 Stormwater Permit: Final Data Characterization 2009-2013. Washington State Department of Ecology, Olympia, WA. Publication No. 15-03-001. https://fortress.wa.gov/ecy/publications/SummaryPages/1503001.html

Howell, J., Coyne, M. S., & Cornelius, P. (1996). Effect of sediment particle size and temperature on Fecal bacteria mortality rates and the Fecal coliform/Fecal streptococci ratio. *Journal of Environmental Quality*, *25*(6), 1216–1220.

Johnsen, A. R., Wick, L. Y. & Harms, H., 2005. Principles of microbial PAH-degradation in soil. *Environmental Pollution*, Volume 133, pp. 71-84.

Kanalay, R.A. and Harayama, S., 2000. Biodegradation of high-molecular-weight polycyclic aromatic hydrocarbons by bacteria. *Journal of bacteriology*, *182*(8), pp.2059-2067.

Kim, M. H., Sung, C. Y., Li, M.-H., & Chu, K.-H. (2012). Bioretention for stormwater quality improvement in Texas: Removal effectiveness of Escherichia coli. *Separation and Purification Technology*, *84*, 120–124.

Kinnaman, A. R., Surbeck, C. Q. & Usner, D. C., 2012. Coliform bacteria: The effect of sediments on decay rates and on required detention times in stormwater BMPs. *Journal of Environmental Protection*, Volume 3, p. 787.

LeFevre, G. H., Novak, P. J., & Hozalski, R. M. (2011). Fate of naphthalene in laboratory-scale bioretention cells: implications for sustainable stormwater management. *Environmental Science & Technology*, *46*(2), 995–1002.

LeFevre, G. H., Novak, P. J., & Hozalski, R. M. (2012). Fate of Naphthalene in Laboratory-Scale Bioretention Cells: Implications for Sustainable Stormwater Management. *Environmental Science & Technology*, *46*(2), 995–1002. https://doi.org/10.1021/es202266z

LeFevre, G. H., Novak, P. J., & Hozalski, R. M. (2015). Effect of Vegetation on the Fate of Petroleum Hydrocarbons in Laboratory-Scale Rain Gardens. In *Low Impact Development Technology: Design Methods and Case Studies* (pp. 37–42).

Li, Y. L., Deletic, A., Alcazar, L., Bratieres, K., Fletcher, T. D., & McCarthy, D. T. (2012). Removal of Clostridium perfringens, Escherichia coli and F-RNA coliphages by stormwater biofilters. *Ecological Engineering*, *49*, 137–145.

Li, Y., McCarthy, D. T., & Deletic, A. (2016). Escherichia coli removal in copper-zeolite-integrated stormwater biofilters: Effect of vegetation, operational time, intermittent drying weather. *Ecological Engineering*, *90*, 234–243.

McLain, J.E., Rock, C.M., Lohse, K. and Walworth, J., 2011. False-positive identification of Escherichia coli in treated municipal wastewater and wastewater-irrigated soils. *Canadian journal of microbiology*, *57*(10), pp.775-784.

McIntyre, J.K., J.W. Davis, C. Hinman, K. H. Macneale, B. F. Anulacion, N. L. Scholz, & J. D. Stark. (2015). Soil bioretention protects juvenile salmon and their prey from the toxic impacts of urban stormwater runoff. *Chemosphere*, *132*, 213–219.

Meador, J. P., Sommers, F. C., Ylitalo, G. M., & Sloan, C. A. (2006). Altered growth and related physiological responses in juvenile Chinook salmon (*Oncorhynchus tshawytscha*) from dietary exposure to polycyclic aromatic hydrocarbons (PAHs). *Canadian Journal of Fisheries and Aquatic Sciences*, *63*(10), 2364–2376. https://doi.org/10.1139/f06-127

Mohanty, S. K., & Boehm, A. B. (2014). Escherichia coli removal in biochar-augmented biofilter: Effect of infiltration rate, initial bacterial concentration, biochar particle size, and presence of compost. *Environmental Science & Technology*, *48*(19), 11535–11542.

Mohanty, S.K., Cantrell, K.B., Nelson, K.L. and Boehm, A.B., 2014. Efficacy of biochar to remove Escherichia coli from stormwater under steady and intermittent flow. *Water research*, *61*, pp.288-296.

Mohanty, S.K., Valenca, R., Berger, A.W., Iris, K.M., Xiong, X., Saunders, T.M. and Tsang, D.C., 2018. Plenty of room for carbon on the ground: Potential applications of biochar for stormwater treatment. *Science of the total environment*, *625*, pp.1644-1658.

Nielsen, K., Kalmykova, Y., Strömvall, A., Baun, A., Eriksson, E. (2015). Particle phase distribution of polycyclic aromatic hydrocarbons in stormwater — Using humic acid and iron nano-sized colloids as test particles. *Science of The Total Environment*, 503: 103-11.

Pagano, T., Bida, M. and Kenny, J.E., 2014. Trends in levels of allochthonous dissolved organic carbon in natural water: a review of potential mechanisms under a changing climate. *Water*, *6*(10), pp.2862-2897.

R Core Team (2020). R: A language and environment for statistical computing. R Foundation for Statistical Computing, Vienna, Austria. URL https://www.R-project.org/.

Rusciano, G. M., & Obropta, C. C. (2007). Bioretention column study: Fecal coliform and total suspended solids reductions. *Transactions of the ASABE*, *50*(4), 1261–1269.

Ryan, J. N., Harvey, R. W., Metge, D., Elimelech, M., Navigato, T., & Pieper, A. P. (2002). Field and laboratory investigations of inactivation of viruses (PRD1 and MS2) attached to iron oxide-coated quartz sand. *Environmental Science & Technology*, *36*(11), 2403–2413.

Selvakumar, A., Borst, M., & Struck, S. (2007). Microorganisms die-off rates in urban stormwater runoff. *Proceedings of the Water Environment Federation*, *2007*(5), 214–230.

Shahsavari, E., Aburto-Medina, A., Taha, M., & Ball, A. S. (2016). A quantitative PCR approach for quantification of functional genes involved in the degradation of polycyclic aromatic hydrocarbons in contaminated soils. *MethodsX*, *3*, 205–211.

Spromberg, J.A., David H. Baldwin, Steven E. Damm, Jenifer K. McIntyre, Michael Huff, Catherine A. Sloan, Nathaniel L. Scholz. (2015). Coho salmon spawner mortality in western U.S.

urban watersheds: bioinfiltration prevents lethal stormwater impacts. *Journal of Applied Ecology*, *53*, 398–407.

Spromberg, J.A., Baldwin, D.H., Damm, S.E., McIntyre, J.K., Huff, M., Sloan, C.A., Anulacion, B.F., Davis, J.W. and Scholz, N.L., 2016. Coho salmon spawner mortality in western US urban watersheds: bioinfiltration prevents lethal storm water impacts. *Journal of Applied Ecology*, *53*(2), pp.398-407.

Taylor, A., Flatt, A., Beutel, M., Wolff, M., Brownson, K. and Stamets, P., 2015. Removal of Escherichia coli from synthetic stormwater using mycofiltration. *Ecological engineering*, *78*, pp.79-86.

Vidovic, S., Block, H.C. and Korber, D.R., 2007. Effect of soil composition, temperature, indigenous microflora, and environmental conditions on the survival of Escherichia coli O157: H7. *Canadian journal of microbiology*, *53*(7), pp.822-829.

(Wa. State Dept. of Ecology, 2019) - Washington State Department of Ecology. Stormwater Management Manual for Western Washington (SWMMWW); Washington State Department of Ecology: Lacey, WA, USA, 2019.

[WAC] Washington Administrative Code. 2020. Freshwater designated uses and criteria Table 200 (2)(b)Primary contact recreation bacteria criteria in freshwater. Olympia (W.A.). WAC 173-201A-200 Table 200 (2)(b). [accessed 2021-03-01]. https://apps.leg.wa.gov/wac/default.aspx?cite=173-201A-200&pdf=true.

Zhang, L., Seagren, E. A., Davis, A. P. & Karns, J. S., 2010. The capture and destruction of Escherichia coli from simulated urban runoff using conventional bioretention media and iron oxide-coated sand. *Water Environment Research,* Volume 82, pp. 701-714.

7 APPENDIX

See Field Report for soil moisture and temperature data, greenhouse conditions, rainfall data, and tabular chemistry and microbiology data.

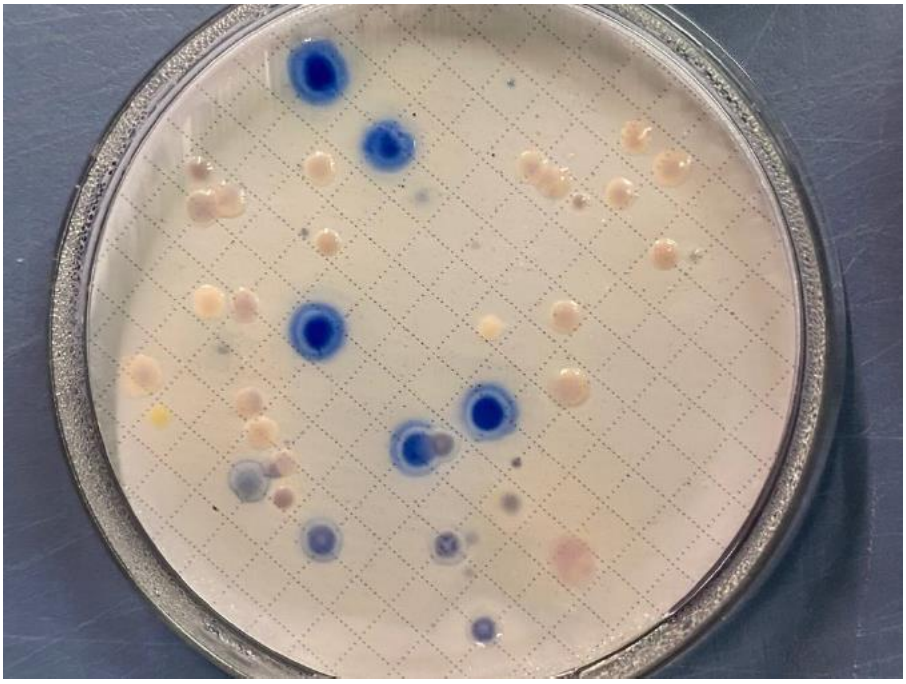

Figure A1. Picture of a fecal coliform membrane filtration growth plate provided by Hillary Eichler from Spectra Laboratories, Tacoma, WA. Blue colonies are fecal coliform, yellow/purple colonies are confluent growth.

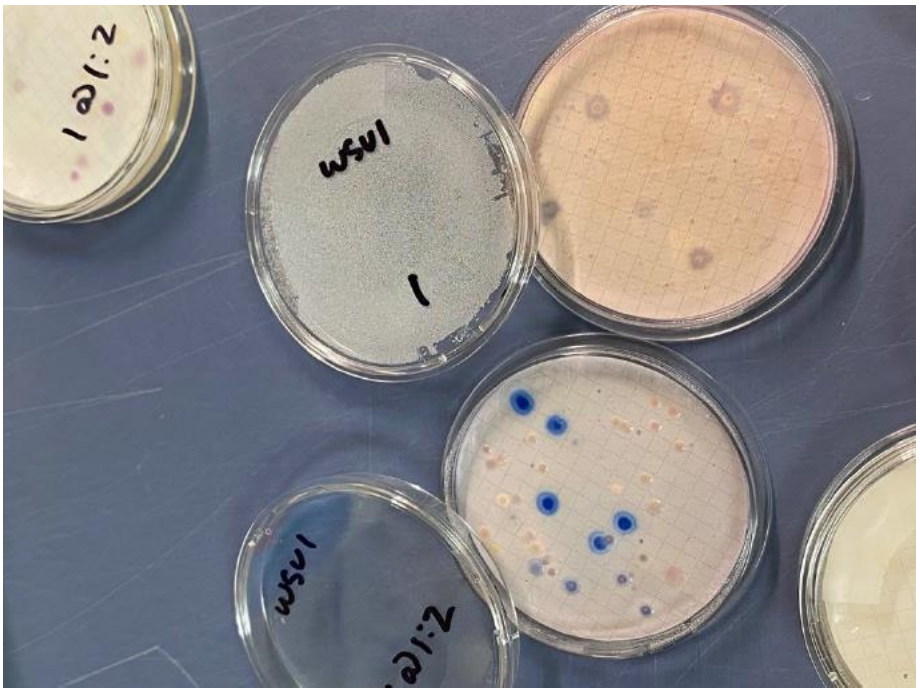

Figure A2. Picture of a fecal coliform membrane filtration growth plate provided by Hillary Eichler from Spectra Laboratories, Tacoma, WA. Blue colonies are fecal coliform, yellow/purple colonies are confluent growth.The top plate shows 1 mL of an undiluted influent sample, while the bottom plate shows a 1 mL of sample that was prediluted by half. In the undiluted top plate, the confluent growth and turbidity have overrun fecal colonies that are in the sample at the 1:2 dilution.

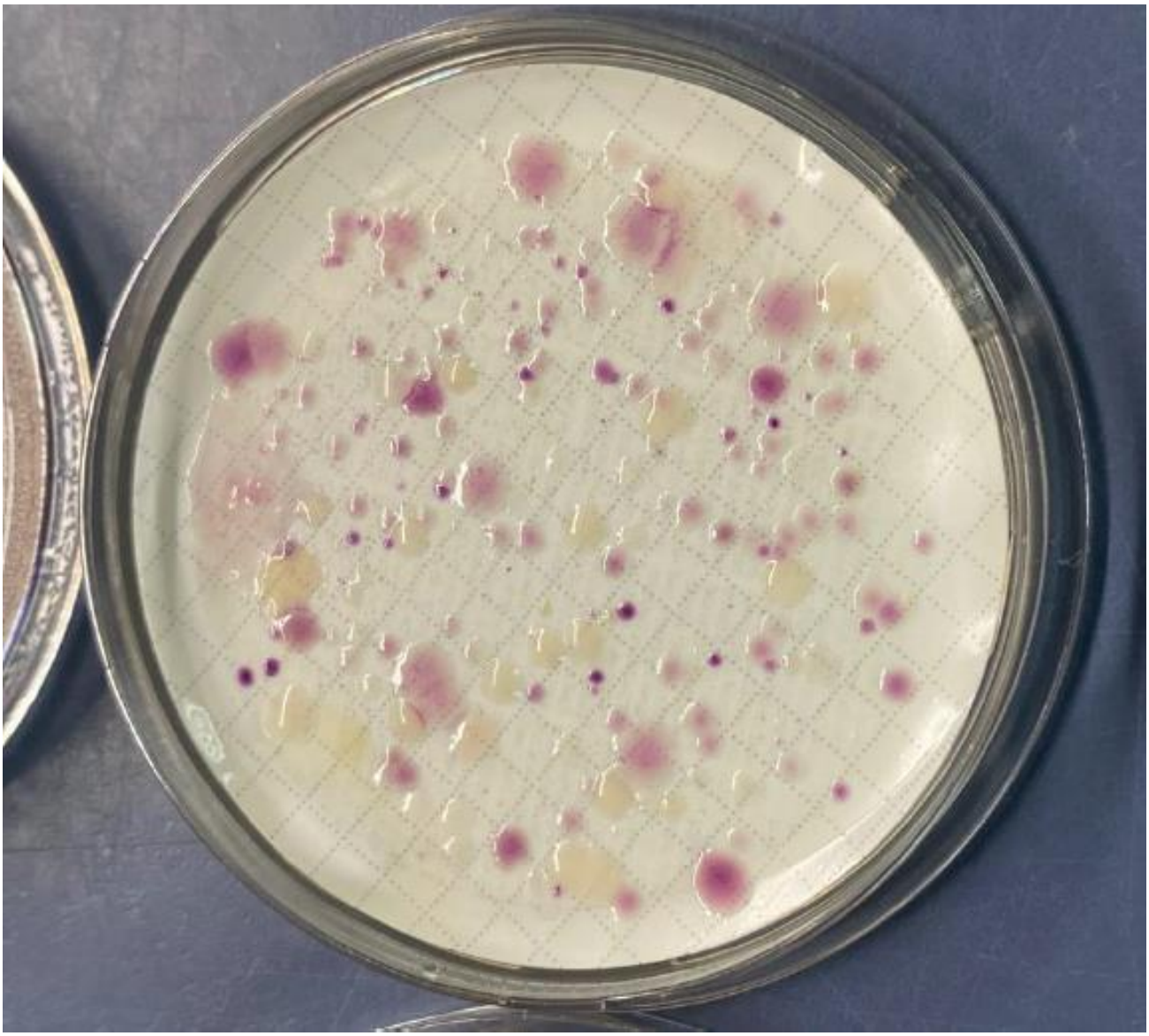

Figure A3. Picture of an *E. coli* membrane filtration growth plate provided by Hillary Eichler from Spectra Laboratories, Tacoma, WA. The purple colonies are *E. coli* and the yellow colonies are confluent growth.

Figure A4. Picture of an *E. coli* membrane filtration growth plate provided by Hillary Eichler from Spectra Laboratories, Tacoma, WA. This plate has more overgrowth than the plate in Figure A3, and the confluent colonies (yellow) are beginning to outperform the *E. coli* colonies (purple).

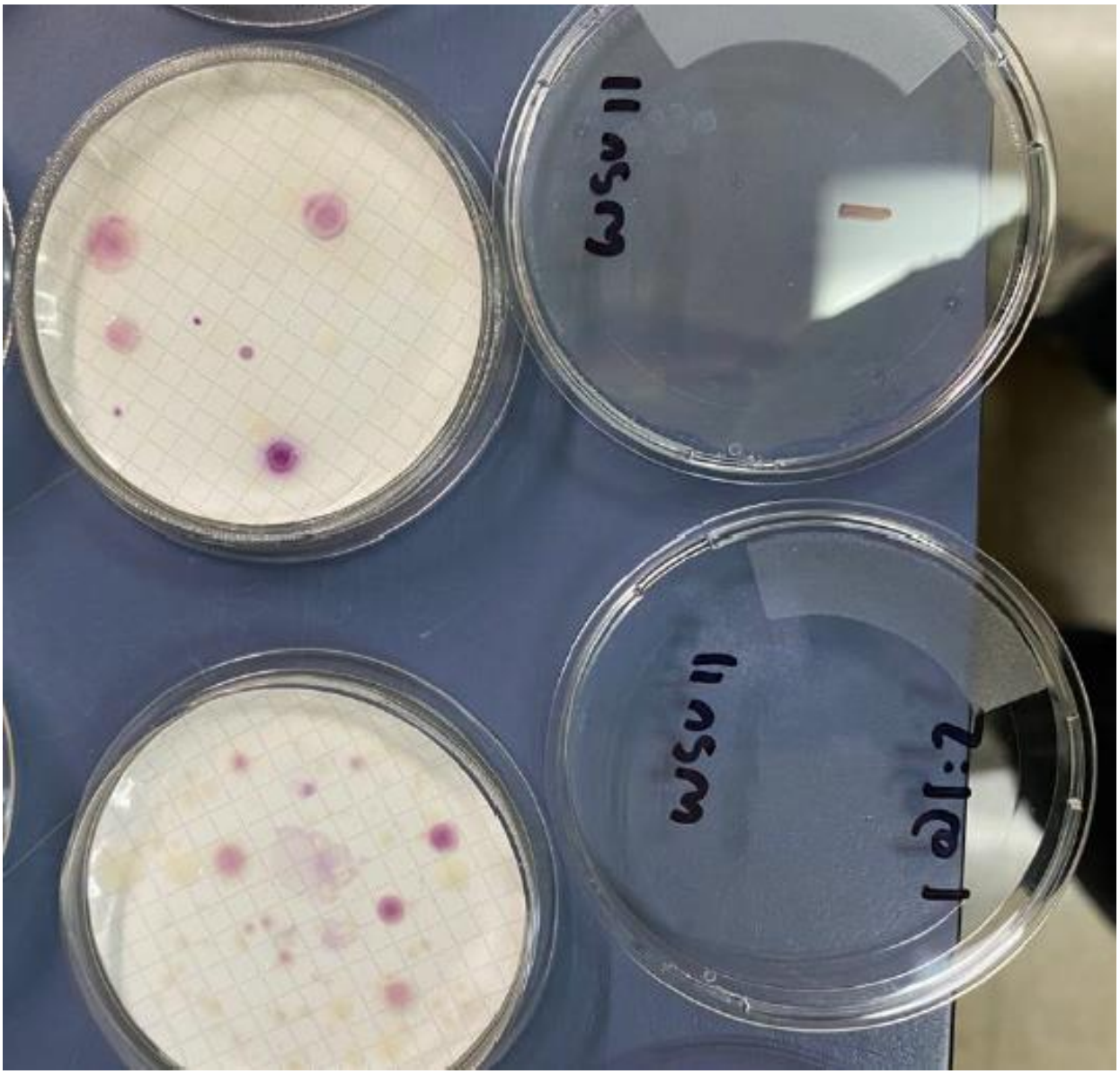

Figure A5. Picture of an *E. coli* membrane filtration growth plate provided by Hillary Eichler from Spectra Laboratories, Tacoma, WA.The top plate contains 1 mL of undiluted sample, while bottom plate contains 1 mL of sample that was prediluted by half. The diluted plate (bottom) has more countable colonies (purple) than the 1 mL plate (top).

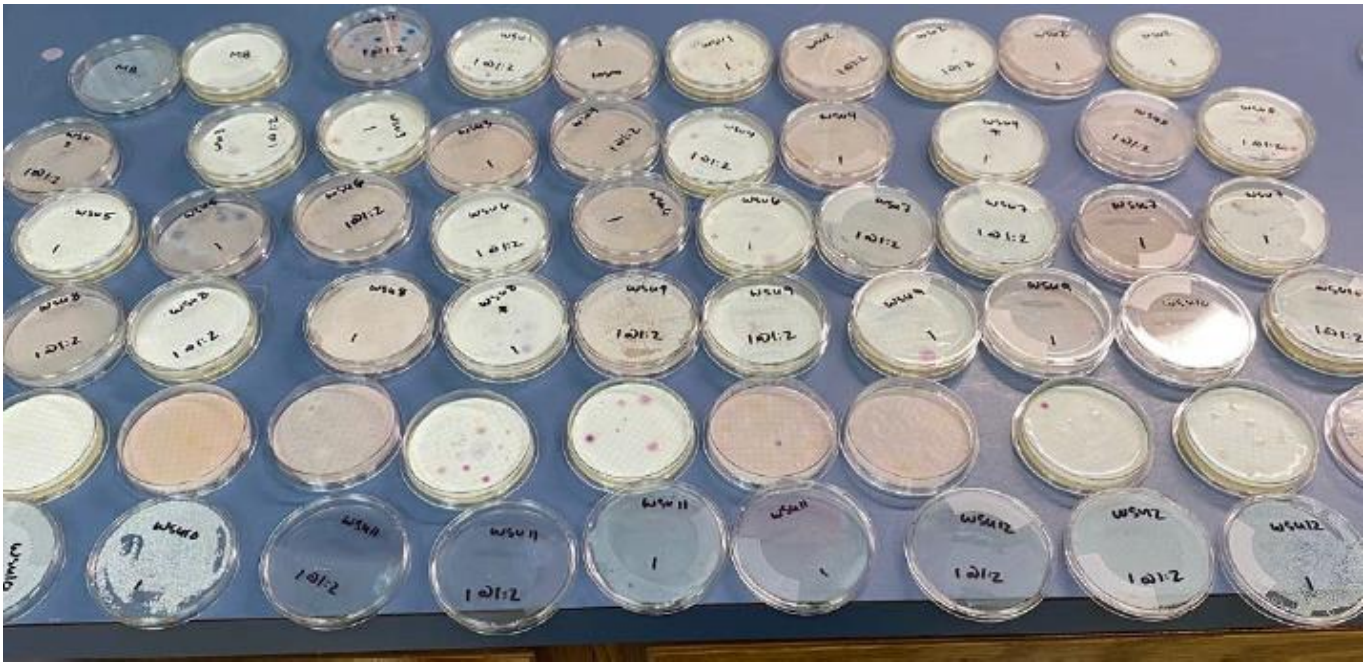

Figure A6. Picture of a set of water samples from dosing event 4 plated on *E. coli* membrane filtration plates. Photos and description were provided by Hillary Eichler from Spectra Laboratories, Tacoma, WA.

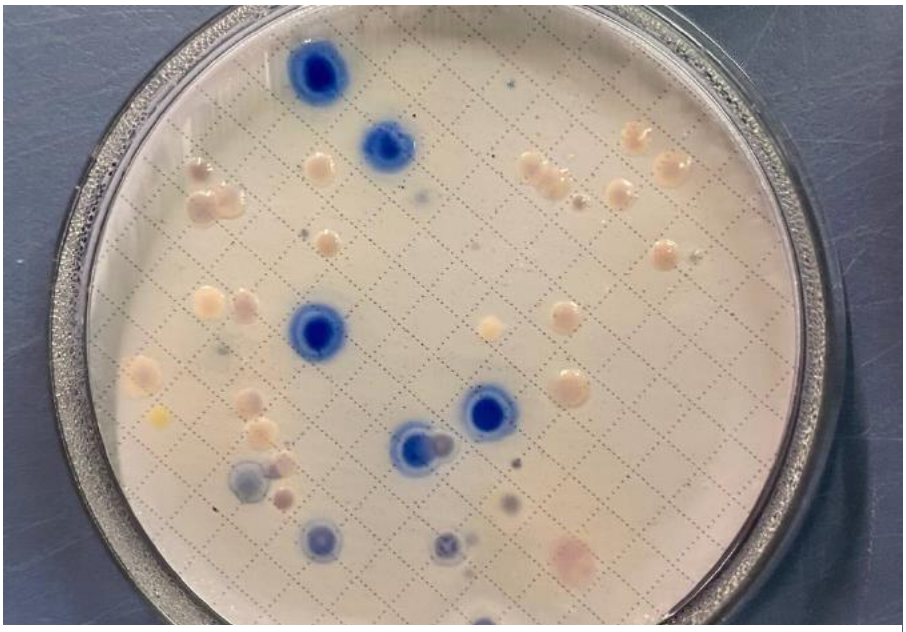

Figure A1. Picture of a fecal coliform membrane filtration growth plate provided by Hillary Eichler from Spectra Laboratories, Tacoma, WA. Blue colonies are fecal coliform, yellow/purple colonies are confluent growth.

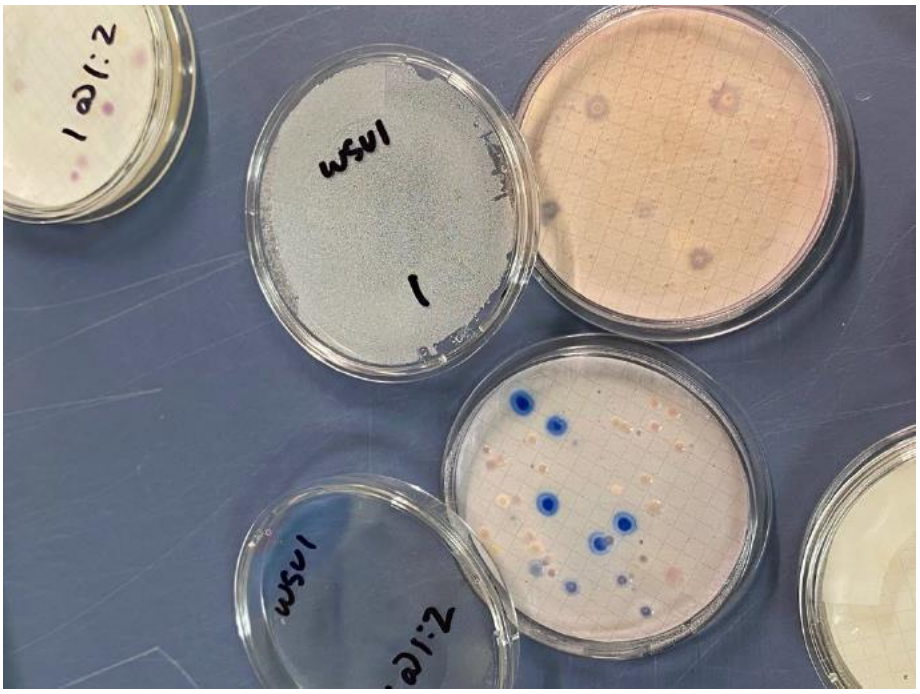

Figure A2. Picture of a fecal coliform membrane filtration growth plate provided by Hillary Eichler from Spectra Laboratories, Tacoma, WA. Blue colonies are fecal coliform, yellow/purple colonies are confluent growth.The top plate shows 1 mL of an undiluted influent sample, while the bottom plate shows a 1 mL of sample that was prediluted by half. In the undiluted top plate, the confluent growth and turbidity have overrun fecal colonies that are in the sample at the 1:2 dilution.

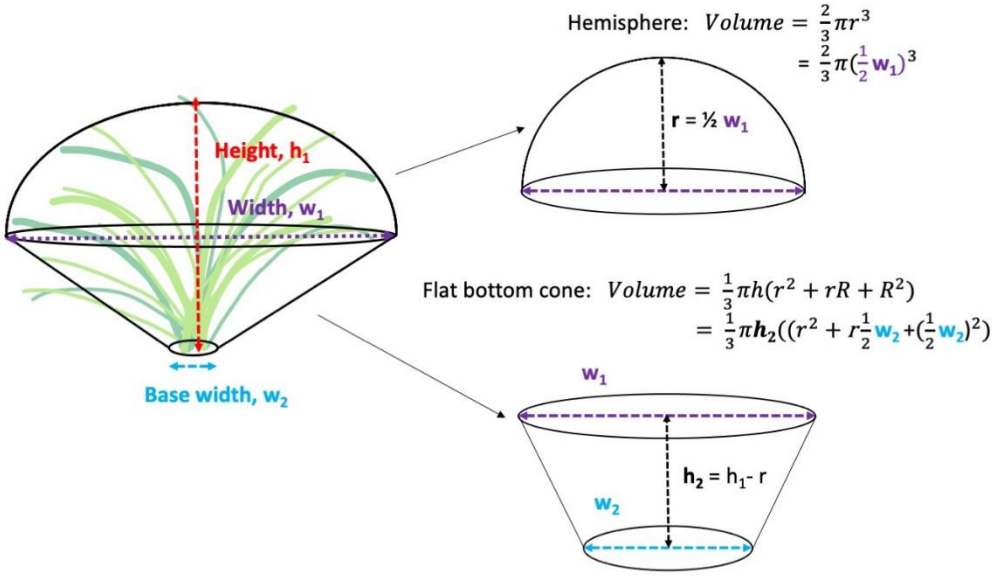

Figure A3. Diagram showing how plant volume was calculated for *Carex oshimensis* using plant height, maxmimum width, and base width.